Report No. CDOT-DTD-R-2000-9

Calculation of Bridge Pier Scour Using The Erodibility Index Method

George Annandale
Steve Smith

March 2001
Final Report

TECHNICAL REPORT DOCUMENTATION PAGE

1. Report No.	2. Government Accession No.	3. Recipient's Catalog No.
CDOT-DTD-R-2000-9		

4. Title and Subtitle	5. Report Date
Calculation of Bridge Pier Scour using the Erodibility Index Method	March 1, 2001
	6. Performing Organization Code

7. Author (s)	8. Performing Organization Report No.
George Annandale and Steve Smith	

9. Performing Organization Name and Address	10. Work Unit No. (TRAIS)
Golder Associates Inc. 44 Union Blvd., Suite 300 Lakewood, Colorado 80228	11. Contract or Grant No. DTFH61-90-C-00000

12. Sponsoring Agency Name and Address	13. Type of Report and Period Covered
Colorado Department of Transportation 4201 E. Arkansas Ave. Denver, Colorado 80222	Final Report September 1995 – March 2001
	14. Sponsoring Agency Code

15. Supplementary Notes

Prepared in cooperation with the U.S. Department of Transportation, Federal Highway Administration

16. Abstract

This report explains the use of the Erodibility Index Method (also known as Annandale's Method) to calculate bridge pier scour. The method can be used to predict scour in any earth material, including rock and cohesive and non-cohesive soils. Earth material properties are represented by a geo-mechanical index that integrates the role of material mass strength, block / particle size, internal shear strength and orientation in quantifying the relative ability of earth material to resist scour. A relationship between the geo-mechanical index and the erosive power of water defines the scour threshold that is used in the scour calculations. By comparing the erosive power that is required to scour an earth material (obtained from the threshold relationship) with the erosive power that is available at the base of a bridge pier, it is possible to calculate scour depth. The report outlines the methods that are used to quantify the geo-mechanical index and those that are used to estimate the erosive power of water flowing around bridge piers, and explains how to calculate scour depth. Application of the method is illustrated with an example.

17. Key Words	18. Distribution Statement
scour, rock, cohesive soil, non-cohesive soil, bridge, piers	No restrictions. This document is available to the public through the National Technical Information Service, Springfield, Virginia 22161

19. Security Classif. (of this report)	20. Security Classif. (of this report)	21. No. of Pages	22. Price
Unclassified	Unclassified	49	

Calculation of Bridge Pier Scour Using The Erodibility Index Method

by

George Annandale
Steve Smith

Report No. CDOT-DTD-R-2000-9

Prepared by
Golden Associates
44 Union Blvd., Suite 300
Lakewood, Colorado 80228

Sponsored by the
Colorado Department of Transportation
In Cooperation with the
U.S. Department of Transportation
Federal Highway Administration

March 2001

Colorado Department of Transportation
Research Branch
4201 E. Arkansas Ave.
Denver, CO 80222
(303) 757-9506

TABLE OF CONTENTS

LIST OF FIGURES

LIST OF FIGURES
(continued)

LIST OF TABLES

LIST OF TABLES
(continued)

INTRODUCTION

This report explains concepts that can be used to understand the scour resistance of earth materials such as rock, slickensided and cohesive clays, and non-cohesive granular material. A semi-empirical approach known as the Erodibility Index Method (Annandale 1995) that can be used to quantify the relative ability of these earth materials to resist scour is presented, concomitantly with a method that can be used to calculate the depth of scour around bridge piers.

The first bridge pier scour analysis using the Erodibility Index was conducted for the Northumberland Strait Bridge (Anglio et al. 1996) (figure 1). This analysis entailed verification of the Erodibility Index Method by using material properties and estimates of the erosive power of water that resulted in scour of rock around one of the bridge piers. Laboratory studies were conducted to quantify the relative magnitude of the erosive power of water around the bridge piers. The verified relationship and estimates of the relative magnitude of the erosive power of water for design conditions were used to predict the likelihood of scour at other bridge piers and to design countermeasures.

Subsequent research on the application of the Erodibility Index Method resulted in a general method to calculate the depth of scour at bridge pier foundations. This report explains the Erodibility Index Method, explains how to apply the method to calculate scour depth around bridge piers, and presents a case study.

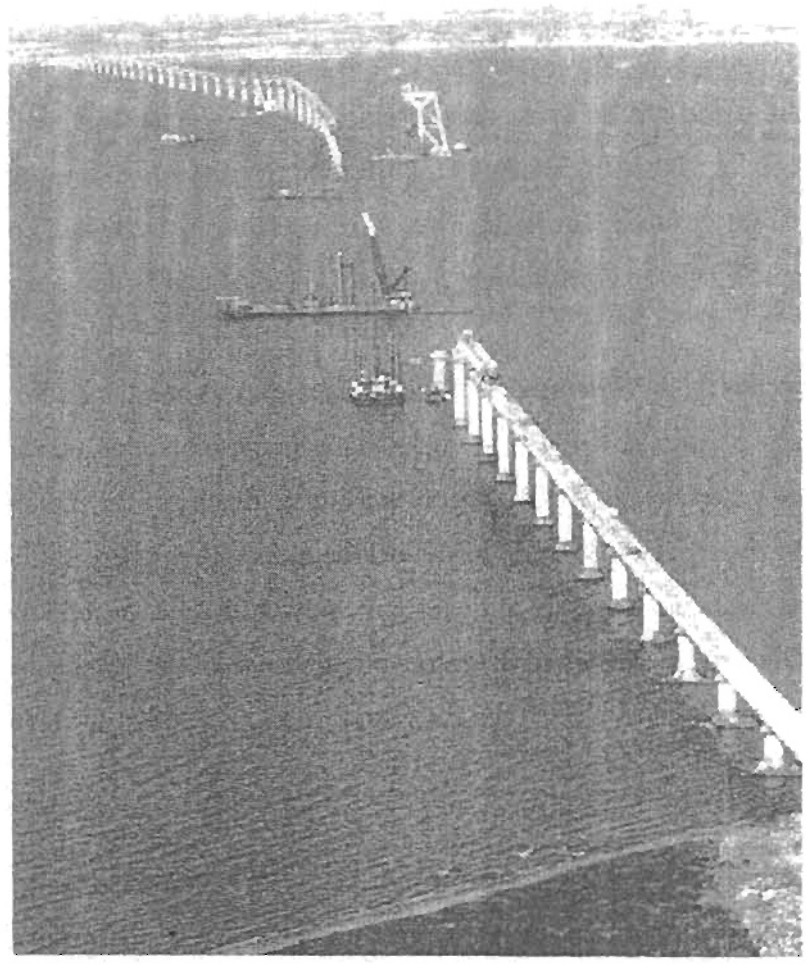

Figure 1. Northumberland Strait Bridge.

ERODIBILITY INDEX METHOD

Development of methods that can be used to predict initiation of scour is challenging and has been the subject of research for many years (e.g. Shields 1936, Hjulstrom 1935, Yang 1973). However, available methods are often limited in their application because they either over-simplify the complexity of the hydraulic processes or they oversimplify the complexity of factors determining the relative ability of earth material to resist scour.

Successful scour models capture the complexity of the behavior of earth materials as well as the essence of the principal processes that quantify the relative magnitude of the erosive power of water. Assumptions that small-scale processes govern the erosion of earth material, often referred to as 'grain-by-grain' removal, can misrepresent actual scour processes because natural earth materials are seldom uniform. The non-uniformity of earth materials is a factor that should be acknowledged when assessing its relative ability to resist erosion. This implies that sole reliance on test results of one parameter, such as undrained shear strength or particle size, can potentially lead to incorrect assessment of the relative ability of earth material to resist scour. Experience has shown that large-scale processes often dominate the scour process (e.g. Annandale 1995, Annandale, et al. 1998, Cohen and Von Thun 1994), and that larger units of earth material may scour prior to grain-by-grain removal. This applies to cases of scour of jointed and fractured rock, and to scour of fissured and slickensided clays. The joints in these materials are often weaker than the crystalline bonds between rock particles or the electro-magnetic bonds created by the Van der Waals forces between clay particles. Failure during the scour process in such cases often proceeds along the discontinuities before the clay or rock blocks, delineated by these discontinuities, break.

The Erodibility Index Method empirically incorporates the principal factors that determine the relative ability of earth material to resist erosion. Conceptual sketches representing the scour process in four material types are presented in figure 2. Figure 2(a) represents a granular

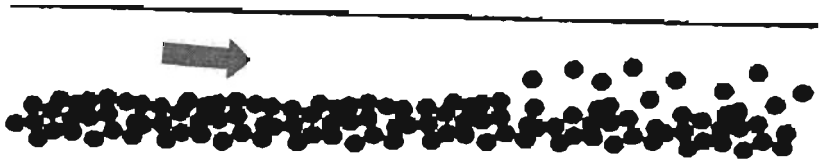

(a) Cohesionless, granular soil.

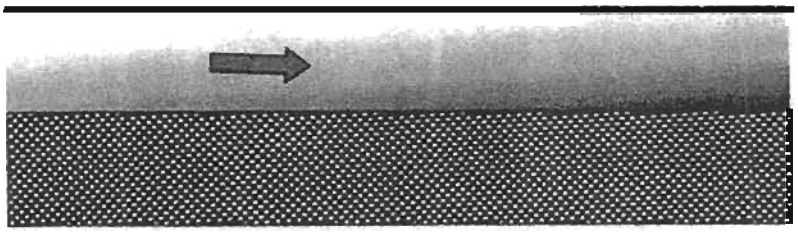

(b) Uniform, cohesive soil.

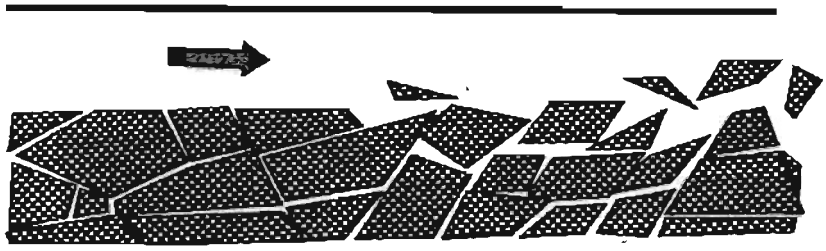

(c) Slickensided clay.

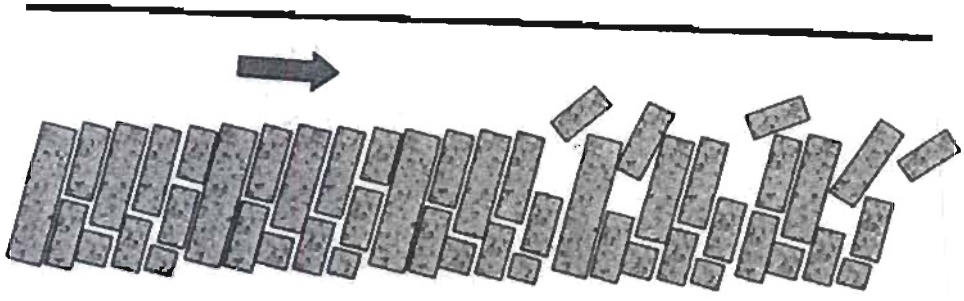

(d) Jointed and fractured rock.

Figure 2. Conceptual representation of erosion for a number of earth material types.

material and figure 2(b) a uniform cohesive soil. A schematic representation of scour in slickensided or fissured clay is presented in figure 2(c), whereas the same for jointed and fractured rock is presented in figure 2(d).

Plucking and cyclic loading introduced by turbulence, most probably the dominant processes in scour of earth materials (Briaud, et al. 1999), act in addition to shear stress to scour earth material. Materials mainly held together by gravity bonds scour principally because of fluctuating forces developing over individual particles, as would be the case for cohesionless granular soil (figure 2(a)). The fluctuating forces pluck the soil particles out of their positions of rest. In the case of uniform cohesive soil, the cyclic loading introduced by the plucking forces weakens the soil, resulting in scour as the soil gradually yields (figure 2(b)).

Consideration of the scour process in more complex materials, such as slickensided or fissured clays, or jointed and fractured rock, indicates that the role of fluctuating pressure is very important. A conceptual model of the scour process in these materials entails the following. When water flows over, say, rock (figure 2(d)), some of the water penetrates the joints and fractures. The pressure caused by the presence of the water between the rock blocks is equal to hydrostatic pressure, determined by the difference between the elevation within the joint and the elevation of the water surface above the joint. Water flowing over the rock is turbulent, resulting in pressure fluctuations at the interface between the rock and the water. The balance between the hydrostatic pressure within the rock fractures and joints, and the fluctuating pressures at the interface results in net fluctuating forces acting on the blocks of rock. The fluctuating pressures move the blocks from their positions of rest, and finally dislodge them. Once dislodged, the water can displace the rock, provided it has enough power. This same concept is applicable to fissured or slickensided cohesive soils, conceptually shown in figure 2(c). Failure is likely to occur along the fractures and joints in the rock, and along the fissures and slickensides in the clay, before failure of the blocks of rock or clumps of clay themselves occur.

Material Resistance

When scour in a complex earth material such as rock is considered, the relative ability of such earth materials to resist erosion is defined by multiple parameters. Material properties that determine scour resistance of rock include intact material strength, block size, shear strength between blocks of rock, and the relative shape and orientation of the rock blocks. By making use of parameters that represent the relative role of each of these properties to resist erosion, it is possible to define a geo-mechanical index that quantifies the relative ability of earth material to resist erosion. Research (Annandale 1995) has shown that the relative ability of other earth materials to resist erosion, such cohesionless silt, sand, gravel and cobbles, and cohesive earth materials, can also be quantified with the same set of parameters as used for rock. The Erodibility Index, which is identical to Kirsten's Excavatability Index (Kirsten 1982), is defined by the equation:

$$K = M_s \cdot K_b \cdot K_d \cdot J_s \tag{1}$$

Where M_s = intact material strength number; K_b = block or particle size number; K_d = discontinuity or inter-particle bond shear strength number; and J_s = relative shape and orientation number. Tables and methods to quantify the constituent parameters are presented in Annandale (1995) and Kirsten (1982).

Erosive Power of Water

The Erodibility Index Method uses stream power, which is equivalent to the rate of energy dissipation in flowing water, to represent the erosive power of water. (These terms are used interchangeably in this report.) By making use of this variable it is possible to quantify the relative magnitude of pressure fluctuations, which play an important role in initiating sediment motion and maintaining sediment transport. In order to support the hypothesis that the rate of energy dissipation can be used to represent the relative magnitude of pressure fluctuations, Annandale (1995) analyzed observations by Fiorotto and Rinaldo (1992) who measured pressure fluctuations under hydraulic jumps. The results of the analysis indicated that the standard deviation of

pressure fluctuations is directly proportional to the rate of energy dissipation (figure 3). This finding supports the use of stream power to quantify the relative magnitude of the erosive power of water. Increases in stream power are related to increases in fluctuating pressures, which form the basis of the conceptual model of the erosion process schematized in figure 2. A method that can be used to determine the magnitude of the rate of energy dissipation around bridge piers is presented further on in this report.

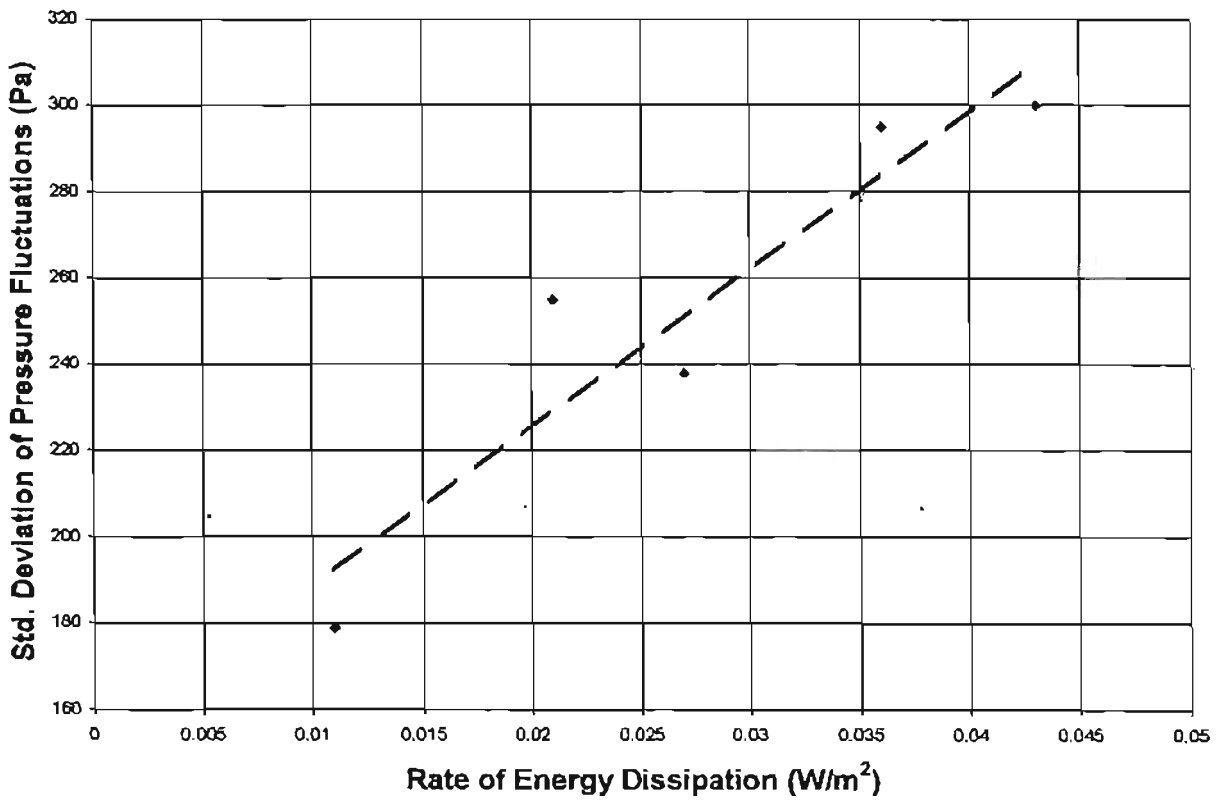

Figure 3. Relationship between the rate of energy dissipation and standard deviation of pressure fluctuations (Annandale 1995).

Erosion Threshold

The correlation between stream power (P) and a mathematical function ($f(K)$) that represents an earth material's relative ability to resist erosion can, at the erosion threshold, be expressed by the relationship:

$$P = f(K) \quad (2)$$

If $P > f(K)$, the erosion threshold is exceeded, and the earth material is expected to erode. Conversely, if $P < f(K)$, the erosion threshold is not exceeded, and the earth material is expected not to erode. The function $f(K)$ represents the Erodibility Index as defined by equation (1).

Annandale (1995) established a relationship between stream power and the Erodibility Index by analyzing published data pertaining to the erosion threshold of cohesionless granular material and field data pertaining to the scour of rock, cohesive soils and vegetated soils. The published data that was used include data by Tison (1953), Gilbert (1914), Kramer (1935), U.S. Army Corps of Engineers, Waterways Experiment Station (WES 1935) and Vanoni (1964). The field data pertaining to the erosion of cohesive soil, vegetated soil and rock was obtained from the Agricultural Research Service (1984 and 1991), Cohen and Von Thun (1994) and van Schalkwyk (1992).

Figure 4 shows the result of the analysis of field data pertaining to scour of cohesive material, vegetated soil, and fractured and jointed rock. Two data types are plotted on the graph, consisting of events where scour occurred and events where scour did not occur. The dotted line indicates the approximate location of the erosion threshold.

Figure 5 contains the results of the analysis of erosion threshold data for cohesionless granular material ranging from silt to sand, gravel, and cobbles. The results plotted on this graph represent the relationship between stream power and the Erodibility Index at the threshold of erosion. Because the relationship is located at the threshold of erosion, the scatter is less than that on figure 4.

If all the data is plotted on one graph (figure 6) the erosion threshold on figure 5 connects with the erosion threshold on figure 4 (the dotted line). The dotted line of figure 4 is not shown on figure 5, due to scale difficulties, but is located at the lower boundary defined by the set of points in the upper right hand part of the figure that represent scour events. It is concluded that the erosion threshold line, as defined by the relationship between stream power and the Erodibility In-

dex, forms a continuous curve for the whole range of earth materials. The earth material represented on figure 5 ranges from silt (at the lower end of the figure) to hard, intact rock (at the upper end of the figure). The erosion threshold lines presented in figures 4 through 6 can be used to determine the erodibility of earth materials and to calculate the extent (depth) of scour. The methods used to achieve these objectives are conceptually discussed in what follows.

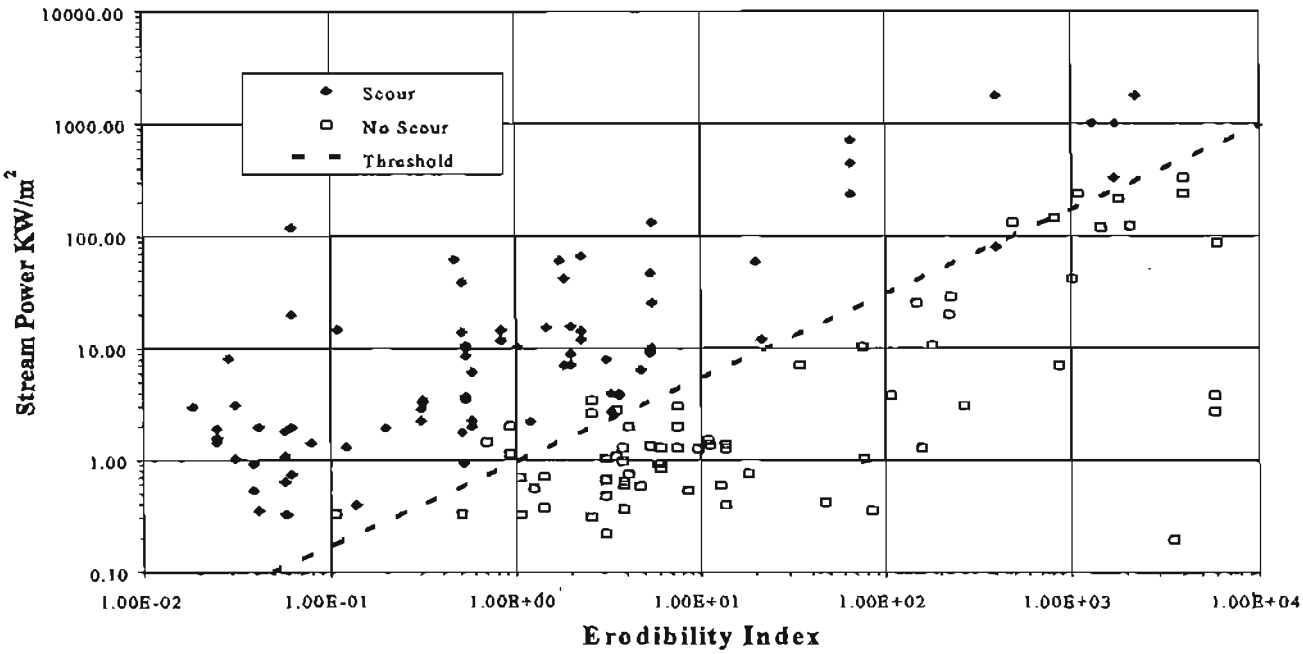

Figure 4. Erosion threshold for higher values of the Erodibility Index (Annandale 1995).

Determination of Erodibility

The erodibility of earth materials is determined by plotting the Erodibility Index for a given earth material and the magnitude of the stream power on figures 4, 5 or 6. If the plotted point is located above the erosion threshold line erosion is expected to occur and if it is located below the threshold line erosion is not expected to occur (figure 7).

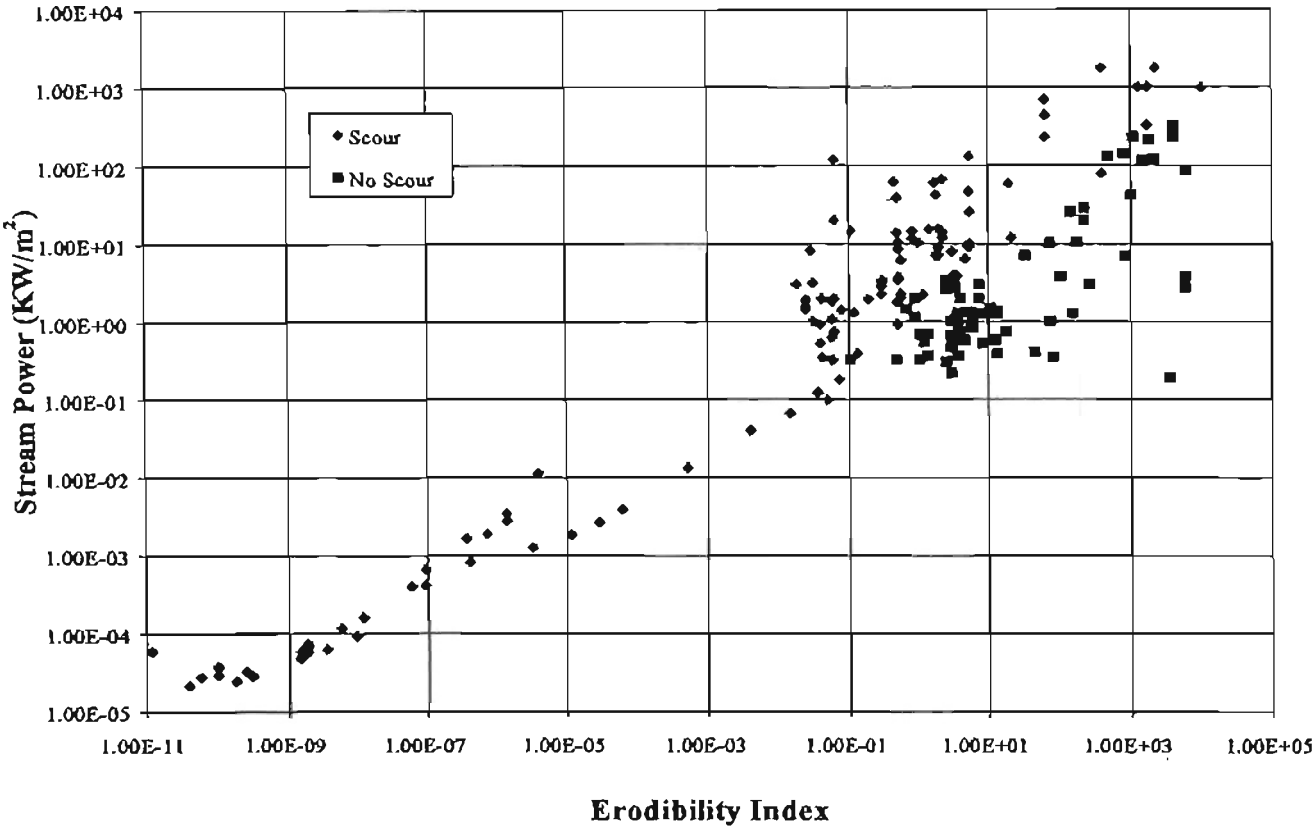

Figure 5. Erosion threshold for lower values of the Erodibility Index (Annandale 1995).

Determination of Extent of Scour

The extent (depth) of scour is determined by comparing the stream power that is *available* to cause scour with the stream power that is *required* to scour the earth material under consideration. The available stream power represents the erosive power of the water discharging over the earth material, whereas the required stream power is the stream power that is required by the earth material for scour to commence. If the available stream power is exactly equal to the required stream power, the material is at the threshold of erosion. In cases where the available stream power exceeds the required stream power, the material will scour. Otherwise, it will remain intact.

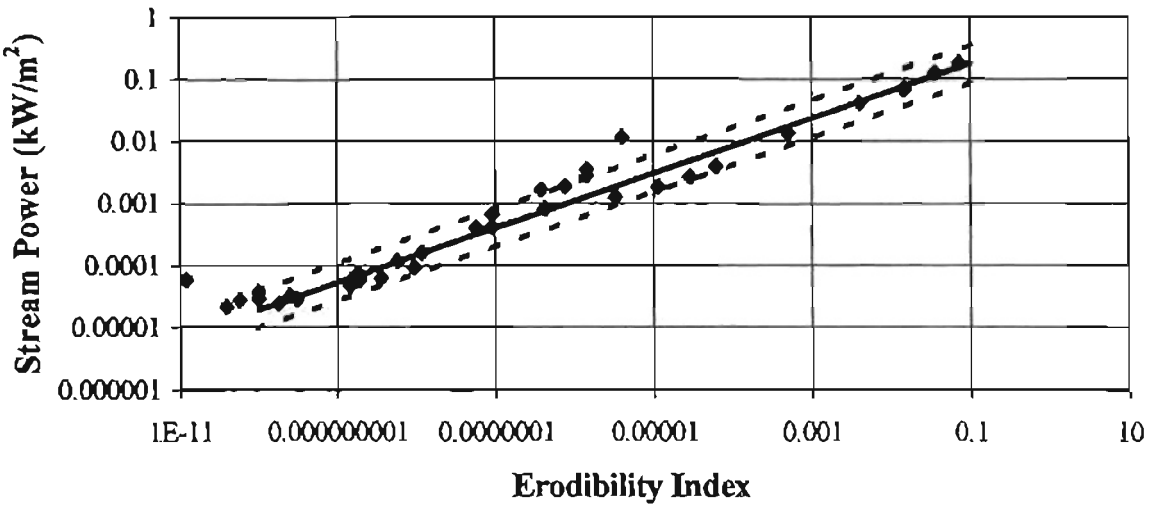

Figure 6. Erosion threshold for the entire range of earth materials, ranging from silt to intact, massive rock – combining figures 4 and 5 (Annandale 1995).

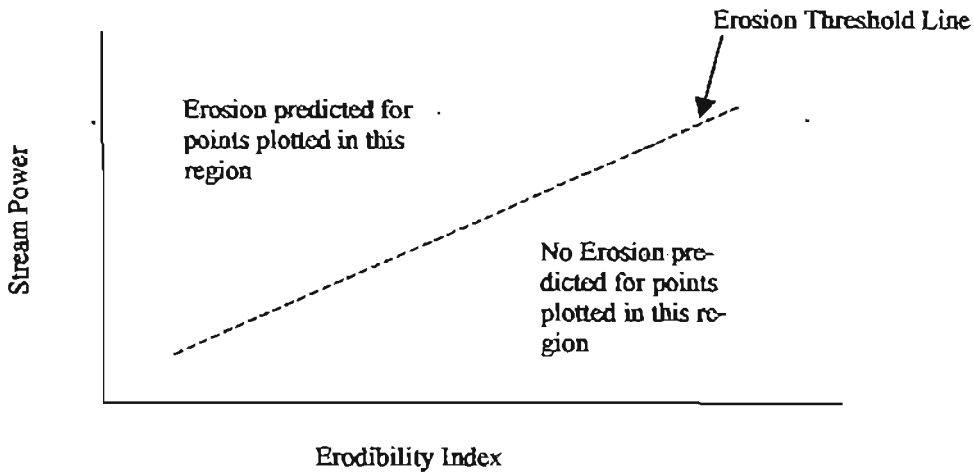

Figure 7. Determination of erodibility of earth materials.

Figure 8 shows how the available and required stream power, both plotted as a function of elevation beneath the riverbed, are compared to determine the extent of scour. Scour will occur when the available stream power exceeds the required stream power. Once the maximum scour elevation is reached the available stream power is less than the required stream power, and scour ceases.

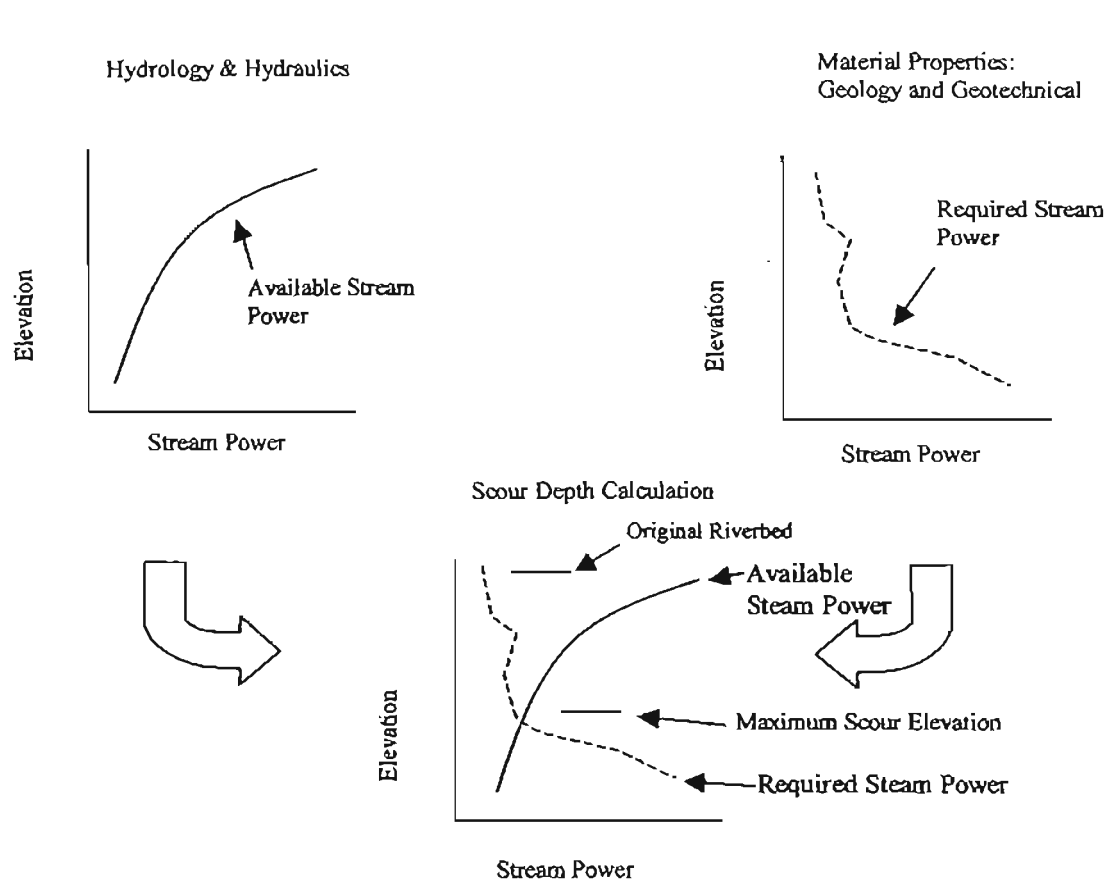

Figure 8. Determination of the extent of scour by comparing available and required stream power.

The required stream power is determined by first indexing a geologic core or borehole data. The values of the Erodibility Index thus determined will vary as a function of elevation, dependent on the variation in material properties. Once the index values at various elevations are known, the required stream power is determined from figure 4 or 6, as conceptually shown in figure 9. Figure 9 indicates that the stream power required to scour a particular earth material is determined by entering the erosion threshold graph on the abscissa, with the Erodibility Index known, moving vertically to the erosion threshold line, and reading the required stream power on the ordinate. Figure 10 illustrates that the process is repeated as a function of elevation below the riverbed. The values of the required stream power is then plotted as a function of elevation.

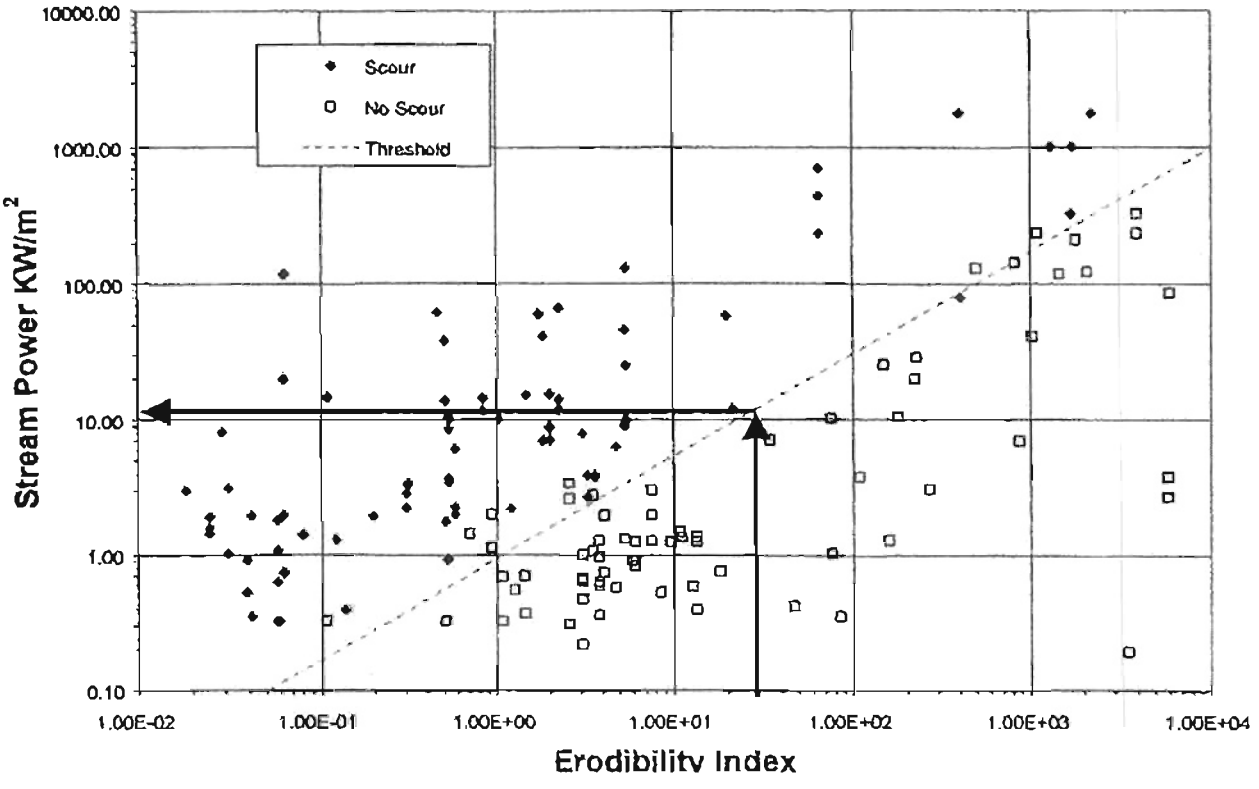

Figure 9. Determination of stream power that is required to scour earth material once the value of the Erodibility Index is known.

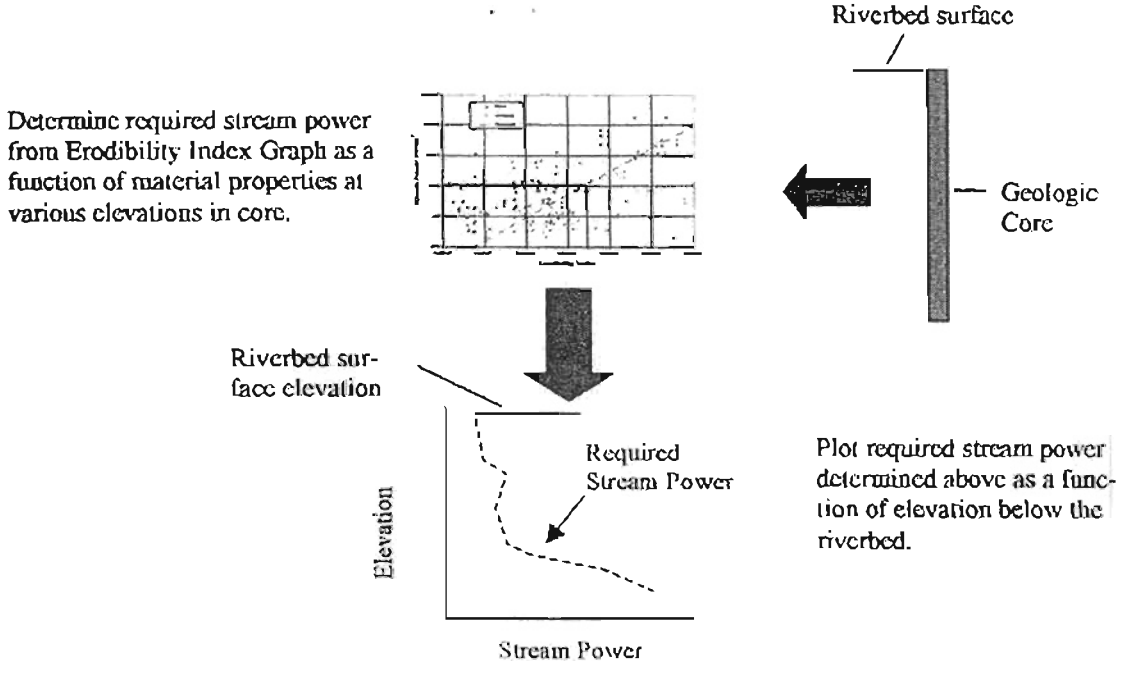

Figure 10. Development of a relationship between the required stream power and elevation below a riverbed.

APPLICATION

Calculation of Stream Power

As water flows around bridge piers, very complex flow patterns develop that increase its turbulence intensity and erosive power. The increase in erosive power of water causes scour around bridge piers that has resulted in the failure of bridges. Research conducted by the Federal Highway Administration (FHWA) (Smith et al. 1997) concluded that the erosive power of water around bridge piers decreases as scour holes increase in depth. This finding has significant implications because earth material often increases in strength as a function of elevation below a riverbed. Concurrent decrease in the magnitude of the erosive power of water and increase in earth material strength cause scour holes around bridge piers to have finite depths. The maximum scour depth occurs at the elevation where the erosive power of water is less than the erosive power that is required to cause scour of the earth material at that elevation.

Estimates of the magnitude of the erosive power of water as a function of scour hole depth can be made by means of physical hydraulic model studies, three-dimensional computer simulation or graphs that are based on the results of the FHWA research (Smith et al. 1997). Figure 11 shows the change in stream power around bridge piers as scour holes increases in depth. The stream power is expressed in dimensionless form as the ratio P/P_a, and scour depth as the dimensionless ratio y_s/y_{max}. P_a is the magnitude of the approach stream power in the river upstream of the pier and P is the magnitude of variable stream power at the base of the scour hole as it increases in depth. The variable y_{max} represents the maximum scour depth for given flow conditions that can develop around a bridge pier without regard to scour resistance offered by earth material, whereas y_s represents variable scour depth ($y_s \leq y_{max}$).

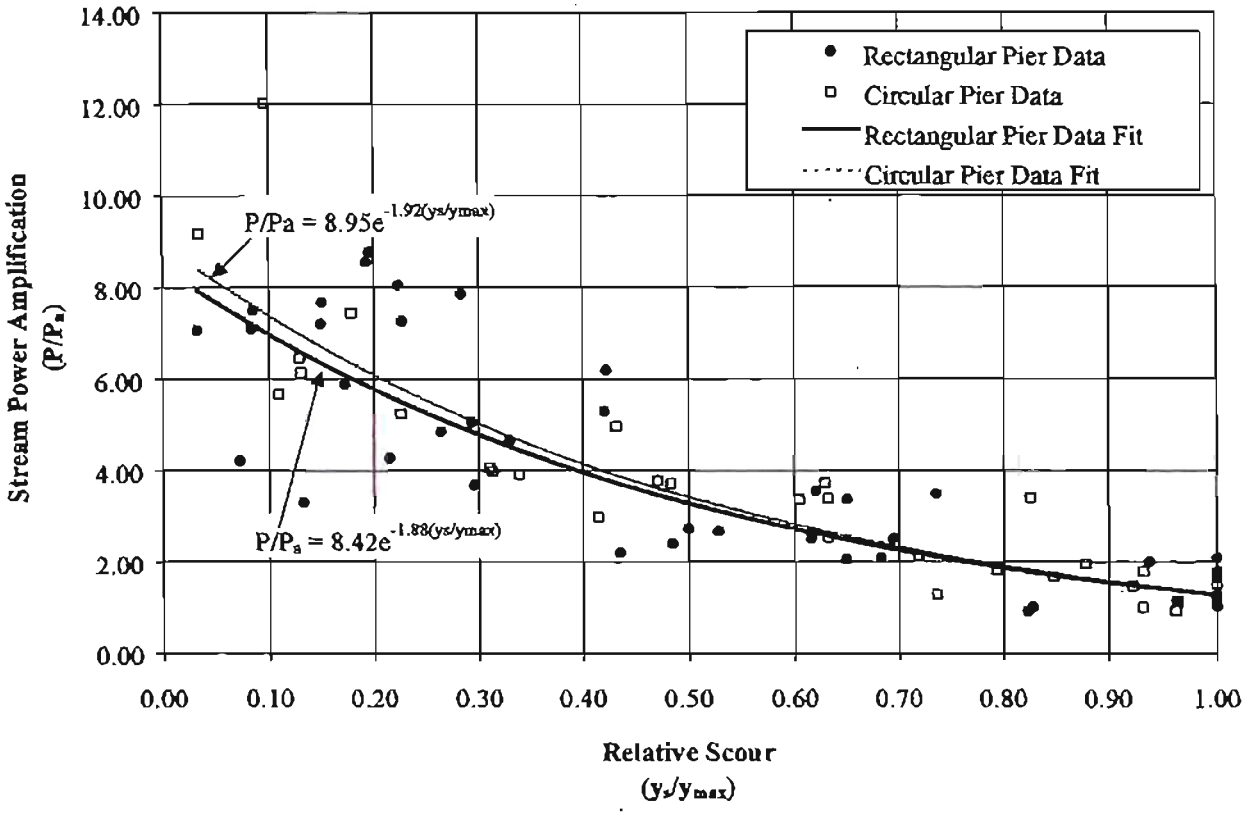

Figure 11. Dimensionless stream power at the base of a scour hole versus dimensionless scour hole depth from FHWA.

Quantification of the axes of figure 11 requires estimates of the approach stream power (P_a) and the maximum scour depth (y_{max}). The equation that is used to calculate the approach stream power is based on the equation derived by Bagnold (1966),

$$P_a = \tau v \tag{3}$$

where P_a = approach stream power per unit area of the bed (W/m^2), τ = shear stress on the bed (N/m^2) and v = velocity (m/s).

By writing shear stress τ as a function of the unit weight of water, flow depth and energy slope, approach stream power can also be expressed as:

$$P_a = \gamma\, d\, s\, v \tag{4}$$

where d = flow depth (m), γ = unit weight of water (N/m^3), s = dimensionless energy slope (or bed slope in the case of uniform, steady flow), and v = velocity (m/s).

An estimate of y_{max} can be obtained by making use of the bridge pier scour equation in HEC-18 (FHWA 1995), which is based on an envelope curve embracing a large number of bridge pier scour experiments. This equation (presented below) is considered to provide a conservative estimate of scour depth.

$$\frac{y_s}{y_1} = 2.0 \cdot K_1 \cdot K_2 \cdot K_3 \cdot \left(\frac{a}{y_1}\right)^{0.65} Fr_1^{0.43} \tag{5}$$

where y_s = scour depth (ft), y_1 = flow depth directly upstream of the pier (ft), K_1 = correction factor for pier nose shape, K_2 = correction factor for angle of attack of flow, K_3 = correction factor for bed condition, a = pier width (ft), L = length of pier (ft), Fr_1 = Froude Number = $V_1/(gy_1)^{1/2}$, and V_1 = mean velocity of flow directly upstream of the pier (ft/s).

With y_{max} assumed to be the maximum scour, the scour depth estimated with the Erodibility Index Method can never exceed this value. The range of scour depth estimates for this method is therefore $0 \leq y_s \leq y_{max}$.

Calculation of the Erodibility Index

The geo-mechanical index that is used by the Erodibility Index Method to quantify the relative ability of earth material to resist erosion was developed by Kirsten (1982) and is expressed as (equation (6)):

$$K = M_s \cdot K_b \cdot K_d \cdot J_s \tag{6}$$

The intact mass strength number (M_s) represents the strength of a homogenous, "perfect" sample of earth material. In order to acknowledge the roles of discontinuities and imperfections for de-

termining the earth material's relative ability to resist scour, the intact mass strength number is multiplied by other parameters. The value of the intact mass strength number is adjusted by multiplying it with the block / particle size number (K_b), the discontinuity / inter-particle bond shear strength number (K_d) and the relative ground structure number (J_s). Ways to quantify each of these numbers are presented in what follows.

Intact Mass Strength of Rock Number

Values of the intact mass strength number (M_s) for cohesionless granular material, cohesive granular material and rock can be found from tables 1 to 3, and can be calculated with equations presented further on in this section.

The values of M_s for **cohesionless** granular soils in table 1 are correlated with field profile identification tests and blow count from the Standard Penetration Test (SPT). The latter is determined in accordance with ASTM D-1586 (Standard Test Method for Penetration Test and Split Barrel Sampling of Soils). Increases in the value of SPT blow counts correspond to increases in the value of M_s. When the SPT blow count exceeds 80, the cohesionless granular material is considered to be equivalent to rock, requiring application of table 3 to quantify the value of M_s. Field identification tests referred to in these tables are in accordance with Korhonen, et al. (1971), Jennings, et al. (1973) and the Geological Society of London (1977).

Vane shear-strength and profile identification data can be used to quantify the value of M_s for **cohesive** soils with the aid of table 2. The vane shear strength is determined in accordance with ASTM D-2573 (Standard Test Method for Field Vane Shear Test in Cohesive Soil) or ASTM D-4648 (Standard Test Method for Laboratory Miniature Vane Shear Test for Saturated Fine-grained Clayey Soil).

Estimates of the undrained shear strength of the cohesive material can also be used if vane shear strength data is unavailable. Such estimates can be made with information obtained from the unconfined compressive strength (UCS) test using ASTM D-2166 (Standard Test Method for Unconfined Compressive Strength for Cohesive Soil).

Table 1. Mass strength number for granular soil (M_s).

Consistency	Identification in Profile	SPT Blow Count	Mass Strength Number (M_s)
Very loose	Crumbles very easily when scraped with geological pick	0-4	0.02
Loose	Small resistance to penetration by sharp end of geological pick	4-10	0.04
Medium dense	Considerable resistance to penetration by sharp end of geological pick	10-30	0.09
Dense	Very high resistance to penetration of sharp end of geological pick – requires many blows of pick for excavation	30-50	0.19
Very dense	High resistance to repeated blows of geological pick – requires power tools for excavation	50-80	0.41
Note: Granular materials in which the SPT blow count exceeds 80 to be taken as rock – see table 3.			

Table 2. Mass strength number for cohesive soil (M_S).

Consistency	Identification in Profile	Vane Shear Strength (kPa)	Mass Strength Number (M_s)
Very soft	Pick head can easily be pushed in up to the shaft of handle. Easily molded by fingers.	0-80	0.02
Soft	Easily penetrated by thumb; sharp end of pick can be pushed in 30 mm – 40 mm; molded by fingers with some pressure.	80-140	0.04
Firm	Indented by thumb with effort; sharp end of pick can be pushed in up to 10 mm; very difficult to mold with fingers. Can just be penetrated with an ordinary hand spade.	140-210	0.09
Stiff	Penetrated by thumbnail; slight indentation produced by pushing pick point into soil; cannot be molded by fingers. Requires hand pick for excavation.	210-350	0.19
Very stiff	Indented by thumbnail with difficulty; slight indentation produced by blow of pick point. Requires power tools for excavation.	350-750	0.41
Note: Cohesive materials of which the vane shear strength exceeds 750kPa to be taken as rock – see table 3.			

Table 3 contains the values of M_s for rock that are related to field identification tests and the unconfined compressive strength (UCS) of the rock, expressed in MPa. The latter can be quantified by making use of the procedures described in ASTM D-2938 (Standard Test Method for Unconfined Compressive Strength of Rock Core Specimens).

Table 3. Mass strength number for rock (M_s).

Hardness	Identification in Profile	Unconfined Compressive Strength (MPa)	Mass Strength Number (M_s)
Very soft rock	Material crumbles under firm (moderate) blows with sharp end of geological pick and can be peeled off with a knife; is too hard to cut tri-axial sample by hand.	Less than 1.7 1.7 – 3.3	0.87 1.86
Soft rock	Can just be scraped and peeled with a knife; indentations 1 mm to 3-mm show in the specimen with firm (moderate) blows of the pick point.	3.3 – 6.6 6.6 – 13.2	3.95 8.39
Hard rock	Cannot be scraped or peeled with a knife; hand-held specimen can be broken with hammer end of geological pick with a single firm (moderate) blow.	13.2 – 26.4	17.70
Very hard rock	Hand-held specimen breaks with hammer end of pick under more than one blow.	26.4 – 53.0 53.00 – 106.0	35.0 70.0
Extremely hard rock	Specimen requires many blows with geological pick to break through intact material.	Larger than 212.0	280.0

The values of M_s for rock can also be quantified by making use of the equations listed below.

$$M_s = C_r \cdot (0.78) \cdot (UCS)^{1.05} \text{ when } UCS \leq 10 \text{ Mpa} \quad (7)$$

and

$$M_s = C_r \cdot (UCS) \text{ when } UCS > 10 \text{ MPa} \quad (8)$$

where C_r = coefficient of relative density. In the case of rock $C_r = g.\rho_r / (27.10^3)$; ρ_r = mass density of the rock in kg/m^3; and g = 9.82 m/s^2, the acceleration due to gravity; 27.10^3 N/m^3 = unit weight of good quality rock.

Weathering will impact values assigned to M_s, especially in the case of rock. Exposed rock can weather during the lifetime of a project, an aspect that might require consideration in some designs. Rock weakens as it weathers with a concomitant decrease in the value of M_s. Assignment of appropriate values of M_s to account for weathering is a matter of professional experience and judgement. It can be accomplished by either testing the strength of samples of weathered rock similar to that under consideration, or by estimating the strength reduction that could be expected, and assigning appropriate M_s values.

Block or Particle Size Number

The block / particle size number (K_b) acknowledges the roles of the sizes of rock block and soil particles in determining earth material resistance to scour. Increases in rock block and particle sizes offer increased resistance to scour.

The value of K_b is determined in different ways for rock and for granular soil. In the case of rock it is a function of rock joint spacing and the number of joint sets, whereas it is a function of particle size in the case of cohesionless granular soil. The value of K_b is set equal to one in the case of fine-grained, homogenous cohesive granular soil.

Rock - Joint spacing and the number of joint sets within a rock mass determine the value of K_b for rock. Joint spacing is estimated from borehole data by means of the rock quality designation (RQD) and the number of joint sets is represented by the joint set number (J_n). RQD is a standard parameter in drill core logging and is determined as the ratio between the sum of the lengths of pieces of rock that are longer than 0.1 m and the total core run length (usually 1.5 m), expressed as a percent (Deere and Deere 1988). RQD values range between 5 and 100. A RQD of 5 represents very poor quality rock, and a RQD of 100 represents very good quality rock. For example, if a core contains four pieces of rock longer than 0.1-m, with lengths of 0.11 m, 0.15 m,

0.2 m and 0.18 m then the cumulative length of rock longer than 0.1 m is 0.64 m and the *RQD* is 0.64 m / 1.5 m x 100 = 43.

Schematic presentations explaining the joint set concept are shown in figure 12 and in the photographs in figures 13 and 14. The values of the joint set numbers (J_n) are found in table 4. J_n is, as can be seen in table 4, a function of the number of joint sets, ranging from rock with no or few joints (essentially intact rock), to rock formations consisting of one to more than four joint sets. The classification accounts for rock that displays random discontinuities in addition to regular joint sets. Random joint discontinuities are discontinuities that do not form regular patterns. For example, rock with two joint sets and random discontinuities is classified as having two joint sets plus random (see table 4). Having determined the values of RQD and J_n, K_b is calculated as:

$$K_b = \frac{RQD}{J_n} \tag{9}$$

where $5 \leq RQD \leq 100$ and $1 \leq J_n \leq 5$.

With the values of *RQD* ranging between 5 and 100, and those of J_n ranging between 1 and 5, the value of K_b ranges between 1 and 100 for rock.

Table 4. Joint set number (J_n).

Number of Joint Sets	Join Set Number (J_n)
Intact, no or few joints/fissures	1.00
One joint/fissure set	1.22
One joint/fissure set plus random	1.50
Two joint/fissure sets	1.83
Two joint/fissure sets plus random	2.24
Three joint/fissure sets	2.73
Three joint/fissure sets plus random	3.34
Four joint/fissure sets	4.09
Multiple joint/fissure sets	5.00

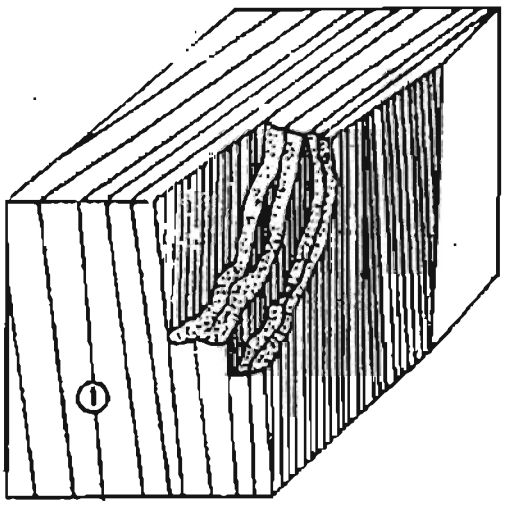

ONE JOINT SET

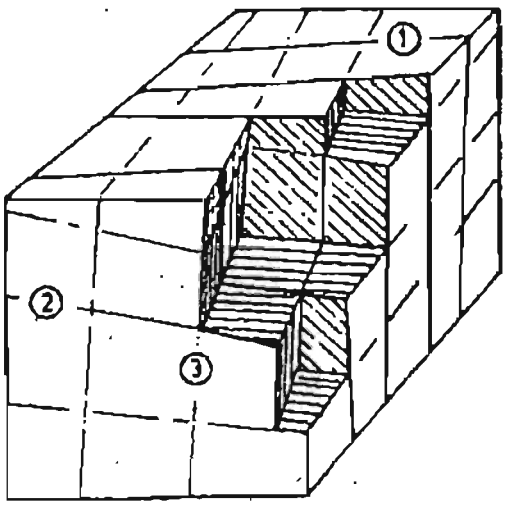

THREE JOINT SET

Figure 12. Schematic presentations illustrating the concept of joint sets.

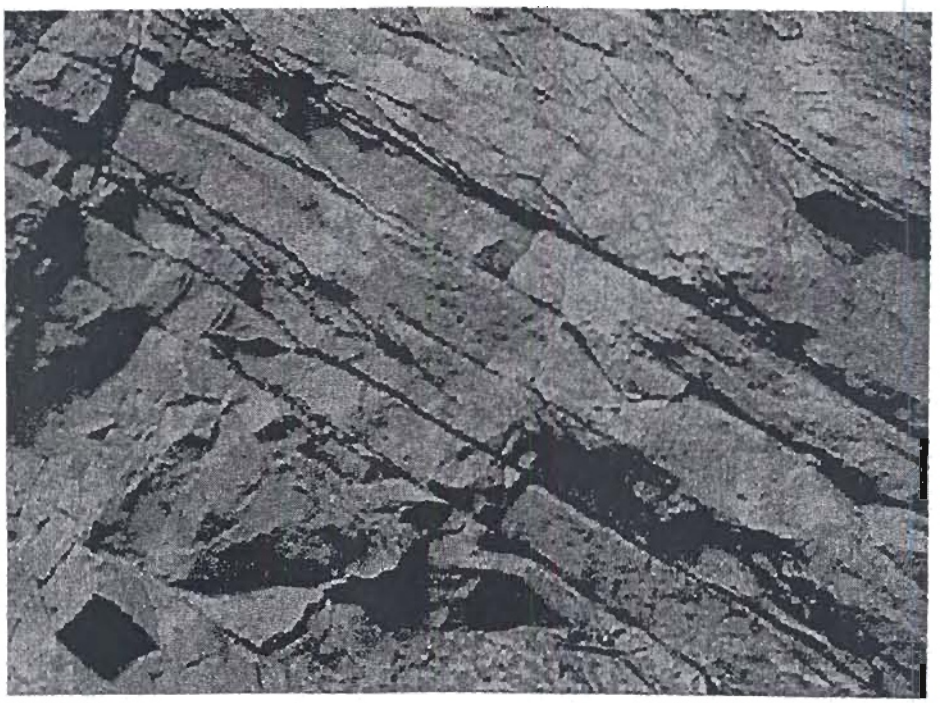

Figure 13. A rock formation with one joint set.

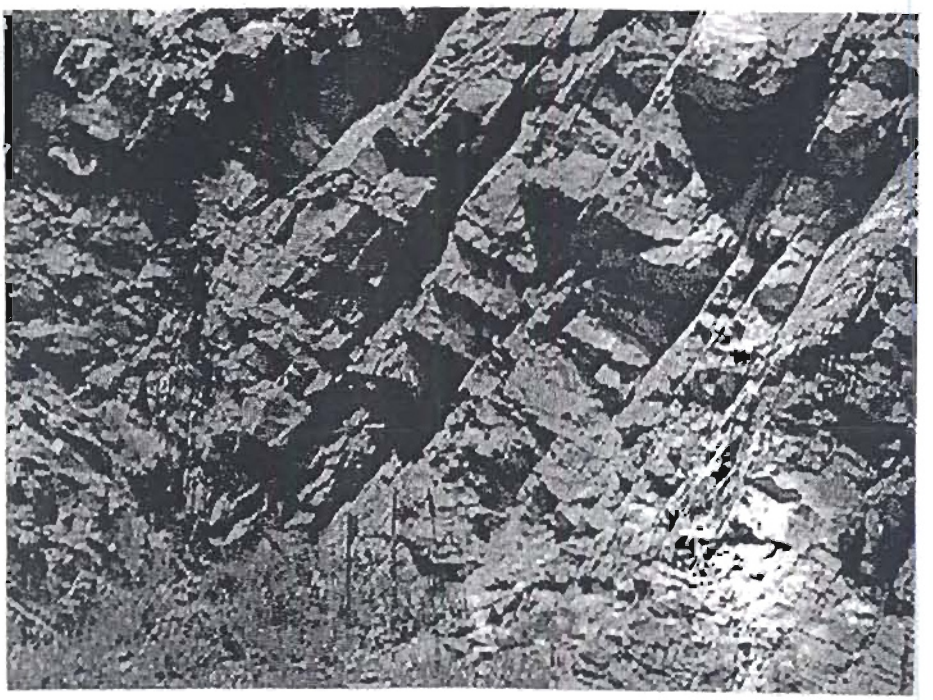

Figure 14. A rock formation with two joint sets.

If RQD data is unavailable, its value can be estimated with one or more of the following equations:

$$RQD = (115 - 3.3 \cdot J_c) \tag{10}$$

J_c is known as the joint count number, a factor representing the number of joints per m^3 of the material, and can also be calculated with the equation,

$$J_c = \left(\frac{3}{D}\right) + 3 \tag{11}$$

where D = mean block diameter in m.

D can be calculated with the equation:

$$D = (J_x \cdot J_y \cdot J_z)^{0.33} \text{ for } D \geq 0.10 \text{ m} \tag{12}$$

Where J_x, J_y and J_z = average spacing of joint sets in m measured in three mutually perpendicular directions, x, y and z. Joint set spacing can be determined by the Fixed Line Survey (see e.g. International Society for Rock Mechanics 1981, Geological Society of London 1977, Bell 1992). In essence, this technique entails measuring the spacing between joints in three orthogonal directions, and averaging the distances for each direction.

Other equations that can be used to calculate RQD, derived from those above, are:

$$RQD = \left(105 - \frac{10}{D}\right) \tag{13}$$

and

$$RQD = \left(105 - \frac{10}{(J_x \cdot J_y \cdot J_z)^{0.33}}\right) \tag{14}$$

Cohesive and Cohesionless, Granular Soils - K_b is set to one ($K_b = 1$) when indexing massive, intact **cohesive** soils. In the case of **cohesionless**, granular soils (including fine, medium, and coarse sands, and gravel and cobbles), the value of K_b is determined by means of the following equation:

$$K_b = 1000 \cdot (D_{50})^3 \text{ for } D_{50} < 0.1 \text{ m} \tag{15}$$

where D_{50} = median particle diameter (m) at the interface between the bed and the water.

The value of D_{50} is determined by standard gradation tests. If the interface between the bed and the water consists of an armor layer, the D_{50} of the armor layer is determined. If the interface does not consist of an armor layer, but an armor layer can potentially form during the scour process, then D_{50} can be set equal to the D_{85} diameter of the gradation of the bed material. The reason for this is that if an armor layer forms during the scour process, then the D_{50} of the armor layer will represent the particle size that protects the underlying bed material. For practical purposes it has been found that the D_{50} of this layer will be approximately equal to the D_{85} of the entire bed material gradation.

Discontinuity / Interparticle Bond Shear Strength Number

The shear strength number, K_d, is calculated differently for rock and granular material. In the case of rock the discontinuity shear strength number is determined as the ratio between two variables representing different characteristics of the surfaces that make up the discontinuity. In the case of granular material, K_d is proportional to the residual angle of friction of the material.

Rock - The discontinuity or inter-particle bond shear strength number (K_d) is the parameter that represents the relative strength of discontinuities in rock and the strength of particle bonding in granular materials. In **rock** it is determined as the ratio between joint wall roughness (J_r) and joint wall alteration (J_a):

$$K_J = \frac{J_r}{J_a} \tag{16}$$

J_r represents the degree of roughness of opposing faces of a rock discontinuity, and J_a represents the degree of alteration of the materials that form the faces of the discontinuity. Alteration relates to amendments of the rock surfaces, for example weathering or the presence of cohesive material between the opposing faces of a joint. Values of J_r and J_a can be found in tables 5 and 6. The values of K_J calculated with the information in these tables change in sympathy with the relative degree of resistance offered by the joints. Increases in resistance are characterized by increases in the value of K_J. The shear strength of a discontinuity is directly proportional to the degree of roughness of opposing joint faces and inversely proportional to the degree of alteration.

Table 5. Joint roughness number (J_r)

Joint Separation	Condition of Joint	Joint Roughness Number
Joints/fissures tight or closing during excavation	Stepped joints/fissures	4.0
	Rough or irregular, undulating	3.0
	Smooth undulating	2.0
	Slickensided undulating	1.5
	Rough or irregular, planar	1.5
	Smooth planar	1.0
	Slickensided planar	0.5
Joints/fissures open and remain open during excavation	Joints/fissures either open or containing relatively soft gouge of sufficient thickness to prevent joint/fissure wall contact upon excavation.	1.0
	Shattered or micro-shattered clays	1.0

Table 6. Joint alteration number (J_a)

Description of Gouge	Joint Alteration Number (J_a) for Joint Separation (mm)		
	1.0[1]	1.0 –5.0[2]	5.0[3]
Tightly healed, hard, non-softening impermeable filling	0.75	-	-
Unaltered joint walls, surface staining only	1.0	-	-
Slightly altered, non-softening, non-cohesive rock mineral or crushed rock filling	2.0	2.0	4.0
Non-softening, slightly clayey non-cohesive filling	3.0	6.0	10.0
Non-softening, strongly over-consolidated clay mineral filling, with or without crushed rock	3.0	6.0**	10.0
Softening or low friction clay mineral coatings and small quantities of swelling clays	4.0	8.0	13.0
Softening moderately over-consolidated clay mineral filling, with or without crushed rock	4.0	8.00**	13.0
Shattered or micro-shattered (swelling) clay gouge, with or without crushed rock	5.0	10.0**	18.0

Note:
[1]Joint walls effectively in contact.
[2]Joint walls come into contact after approximately 100-mm shear.
[3]Joint walls do not come into contact at all upon shear.
**Also applies when crushed rock occurs in clay gouge without rock wall contact.

Joint roughness is described by referring to both large and small-scale characteristics. The large-scale features are known as stepped, undulating or planar; whereas the small-scale features are referred to as rough, smooth or slickensided. Examples of planar and undulating joints are shown in figure 15 and figure 16 respectively. Figure 17 is a schematic presentation of conventional descriptions of joint roughness.

A planar, rough joint indicates that the large-scale feature is planar, but that the joint surfaces are rough. The concept of closed, open and filled joints, terminology used in table 5, is illustrated in figure 15. The value of K_a that is calculated by means of equation (16) is roughly equal to the tangent of the residual angle of friction between the rock surfaces.

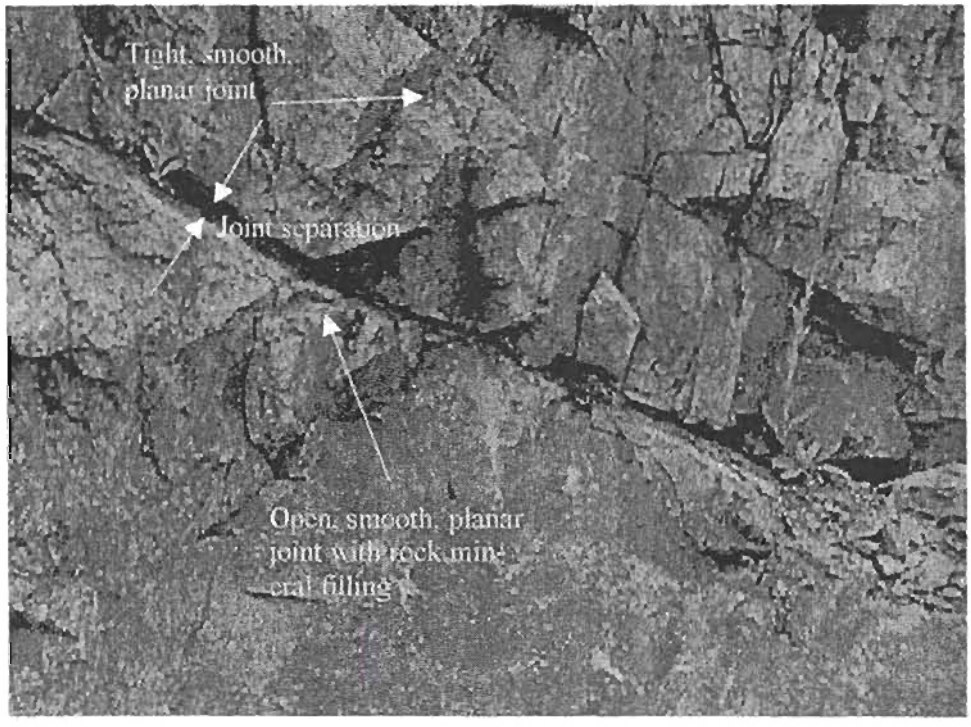

Figure 15. Planar joints.

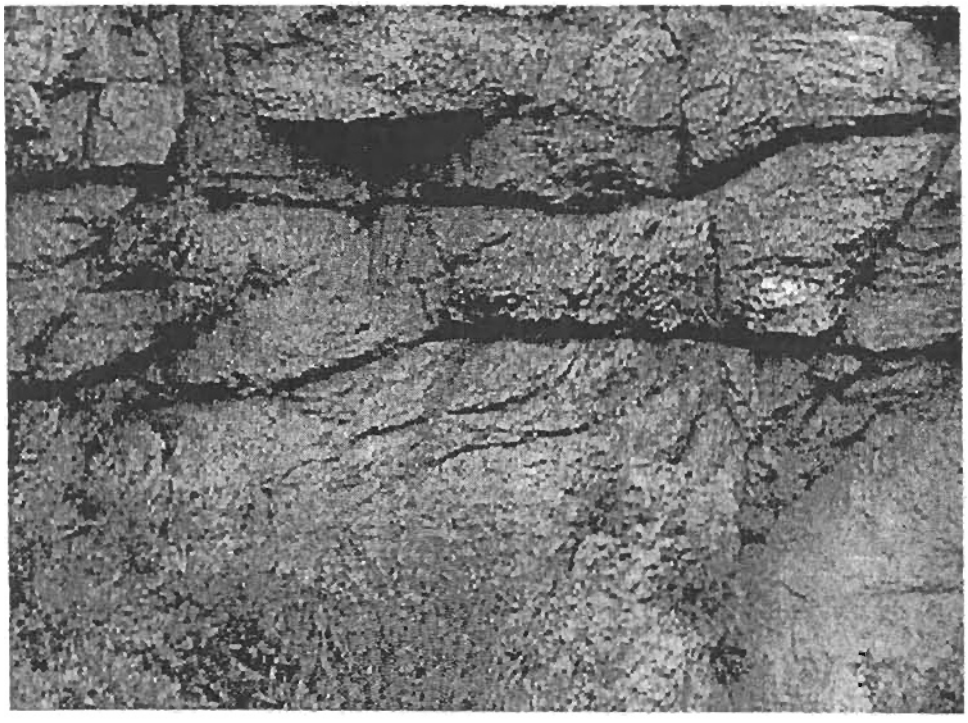

Figure 16. Undulating joints.

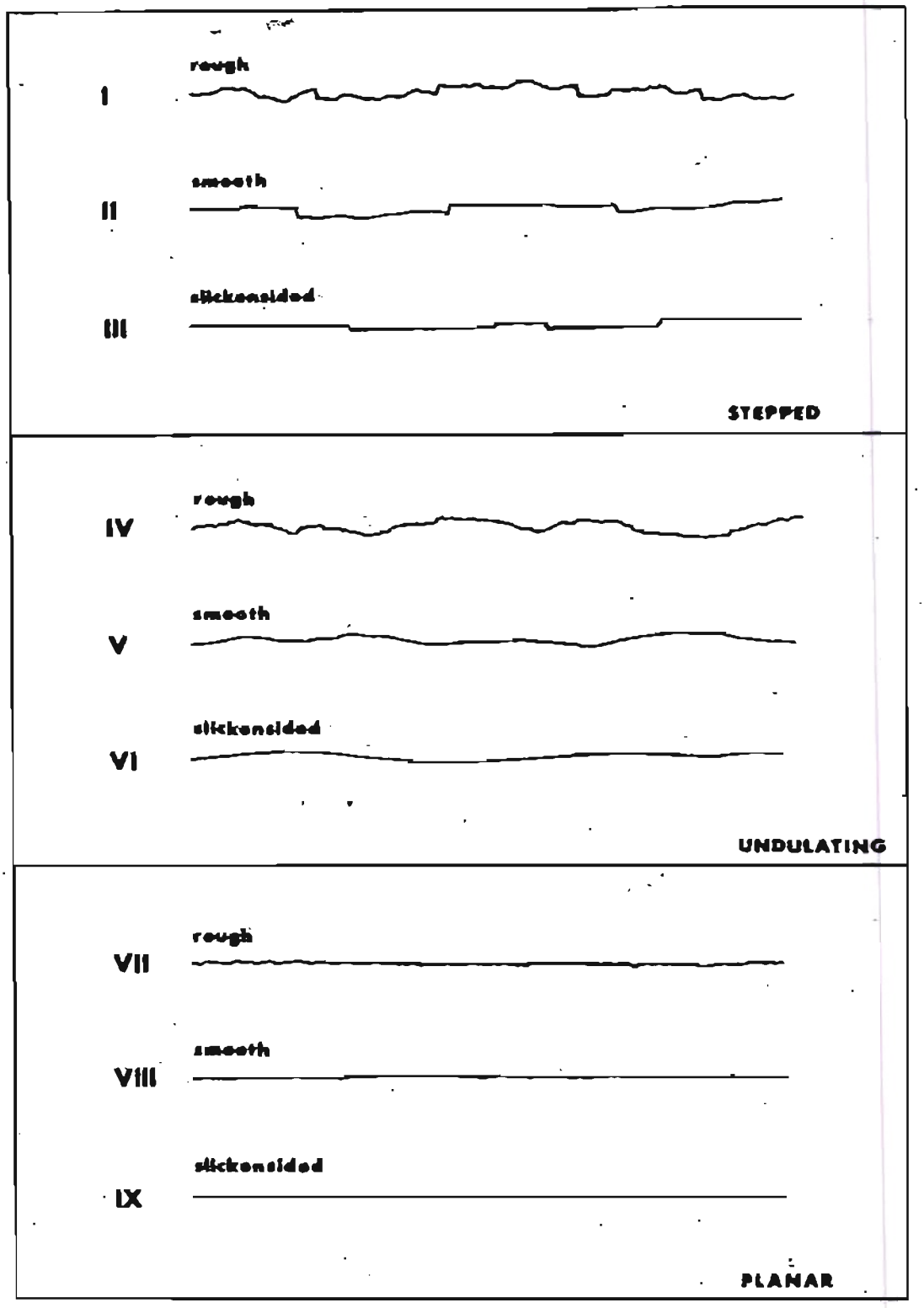

Figure 17. Schematic presentation of conventional descriptions of joint roughness.

Cohesive and Cohesionless Granular Earth Material - In granular materials the inter-particle bond strength number is estimated by the following equation:

$$K_d = \tan\phi \tag{17}$$

where ϕ = residual friction angle of the granular earth material.

Relative Ground Structure Number

The relative ground structure number (J_s) represents the relative ability of earth material to resist erosion due to the structure of the ground. This parameter is a function of the dip and dip direction of the least favorable discontinuity (most easily eroded) in the rock with respect to the direction of flow, and the shape of the material units. These two variables (orientation and shape) affect the ease by which the stream can penetrate the ground and dislodge individual material units.

The concepts of dip and dip direction of rock are illustrated in figure 18. This figure shows a perspective view of a block of rock with a slanting discontinuity. The line that is formed where the horizontal plane and the plane of the discontinuity intersect is known as the strike of the rock. The dip direction, measured in degrees azimuth, is the direction of a line in the horizontal plane that is perpendicular to the strike and located in the vertical plane of the dip of the rock. The dip of the rock is the magnitude of the angle between the horizontal plane and the plane of the discontinuity, measured perpendicular to the strike. If the flow direction is roughly in the same direction as the dip direction, then the dip is said to be in the direction of the flow. If the flow direction is opposite to the dip direction, then the dip is said to be opposite to the direction of flow.

The shape of rock blocks is quantified by determining the joint spacing ratio (r), which is the quotient of the average spacing of the two most dominant high angle joint sets in the vertical plane – see figure 19.

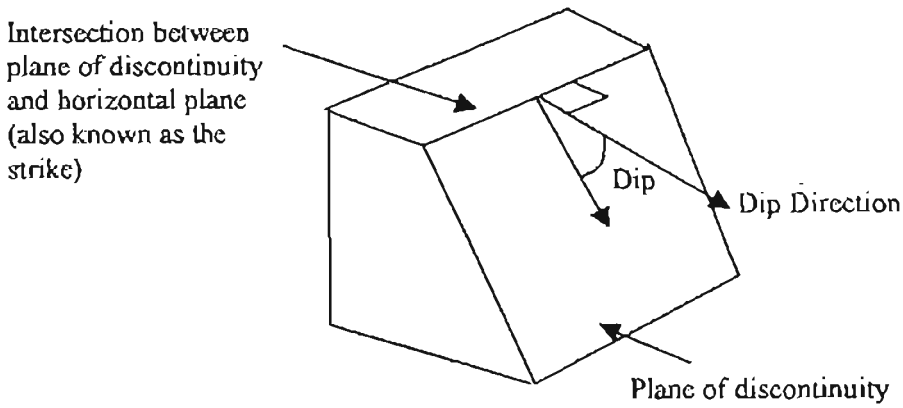

Figure 18. Definition sketch pertaining to dip and dip direction of rock.

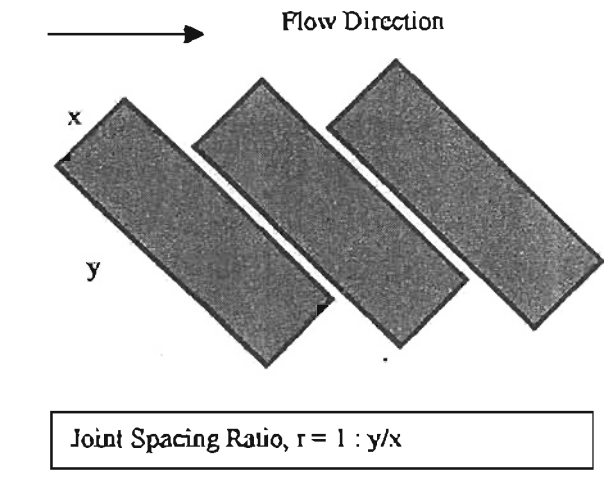

Figure 19. Determination of the joint spacing ratio, *r*.

Conceptually the function of Relative Ground Structure Number (J_s), incorporating shape and orientation, is as follows. If rock is dipped against the direction flow, it will be more difficult to scour the rock than when it is dipped in the direction of flow. When it is dipped in the direction of flow, it is easier for the flow to lift the rock, penetrate underneath and remove it. Rock that is dipped against the direction of flow will be more difficult to dislodge (figure 20).

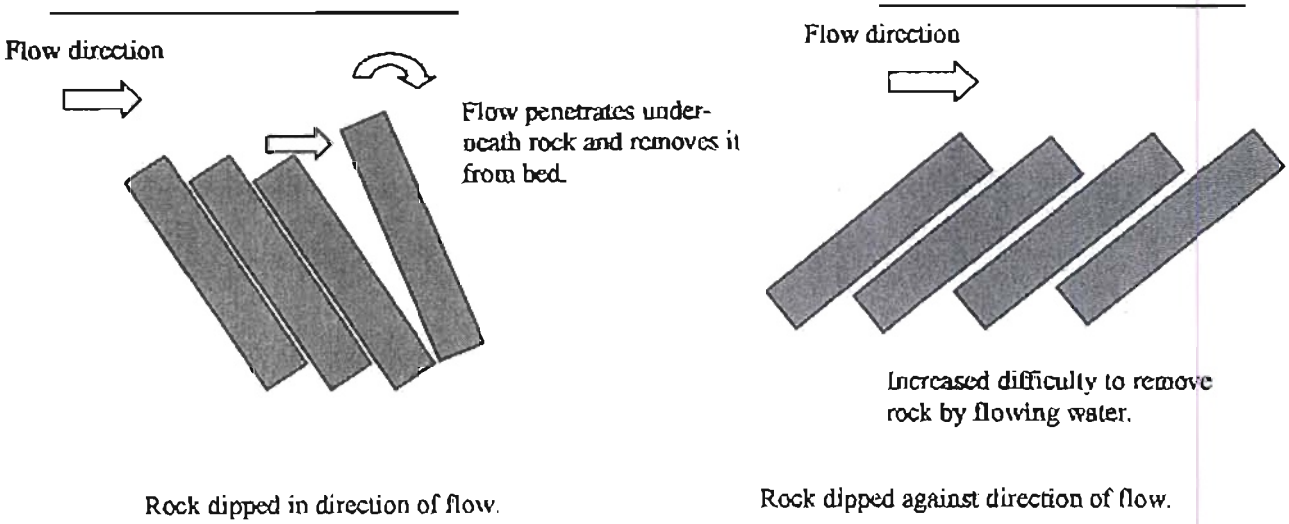

Figure 20. Influence of dip direction on scour resistance offered by rock.

The shape of the rock, represented by the ratio r, impacts the erodibility of rock in the following manner. Elongated rock will be more difficult to remove than equi-sided blocks of rock (figure 21). Therefore, large ratios of r represent rock that is more difficult to remove because it represents elongated rock shapes.

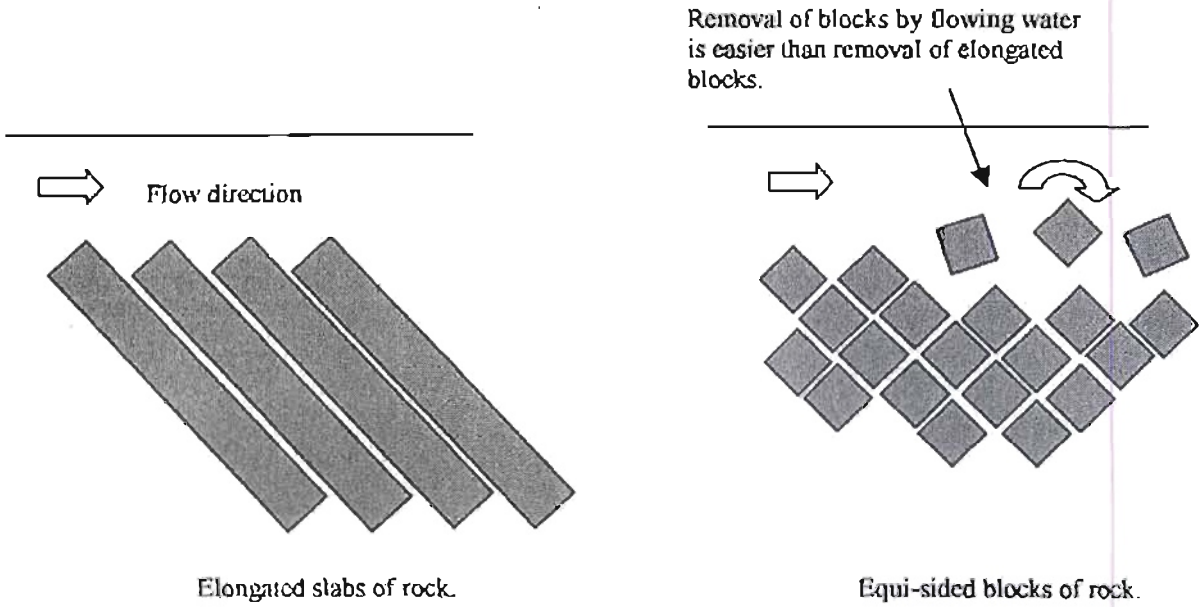

Figure 21. Influence of shape of rock blocks on scour resistance.

The dip of the least favorable discontinuity with respect to the direction of flow is determined by the procedure outlined below. The variables that are used in the calculation include flow direction (*FD*), true dip (*TD*), dip direction (*DD*), ground slope (*GS*) and strike. The descriptions of these variables should be considered concurrently with figure 22, representing the horizontal plane, and figure 23, representing the vertical plane:

- The flow direction (*FD*) is the dominant direction of flow projected on a horizontal plane, expressed as an azimuth angle $(0^\circ \le FD \le 360^\circ)$.
- The ground slope (*GS*) is an angle measured from the horizontal in the vertical plane associated with the flow direction $(0^\circ \le GS \le 90^\circ)$.
- The dip direction (*DD*) is a vector that is perpendicular to the strike of the least favorable (most easily eroded) joint set, expressed as an azimuth angle $(0^\circ \le DD \le 360^\circ)$(this angle also referred to as the *trend*).
- The true dip (*TD*), also called the *plunge*, of the least favorable joint set $(0^\circ \le TD \le 90^\circ)$ is measured in the vertical plane associated with the dip direction.
- The strike is perpendicular to the dip direction, as shown in figure 22.

The procedure is to first calculate the apparent dip (*AD*) and then the effective dip (*ED*). The apparent dip is the dip of the least favorable discontinuity with respect to the flow direction (*FD*). The effective dip (*ED*) is the difference between the apparent dip (*AD*) and the ground slope (*GS*). The value of the effective dip is used in table 7, concurrently with the value of the joint spacing ratio r, to determine the value of J_s.

The apparent dip (*AD*) is determined from the true dip through the use of the following equation:

$$\tan(AD) = \tan(TD) * |\sin(\text{strike} - FD)| \tag{18}$$

If the flow direction is in the direction of the true dip, $(|DD\text{-}FD| < 90^\circ)$ or $(|DD\text{-}FD| > 270^\circ)$, the effective dip (*ED*) is determined by subtracting the ground slope from the apparent dip:

$$ED = AD\text{-}GS \tag{19}$$

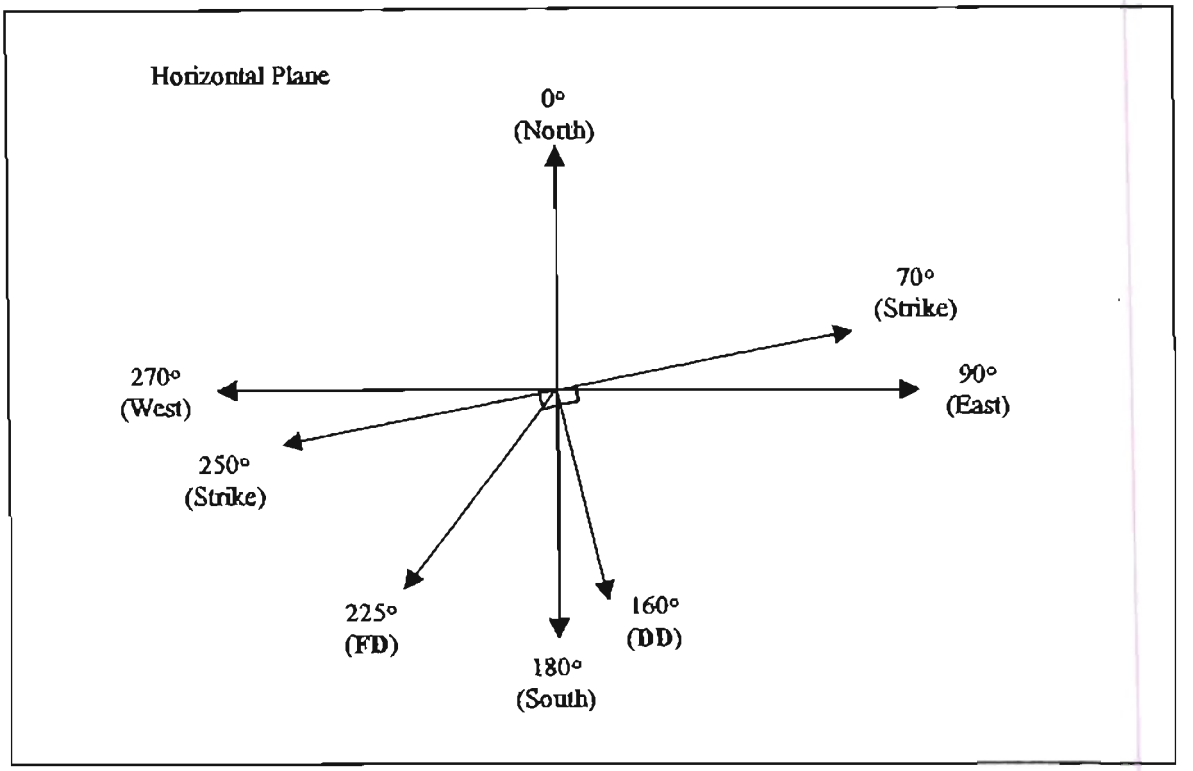

Figure 22. Horizontal plane showing relationships between flow direction (*FD*), dip direction (*DD*) and strike.

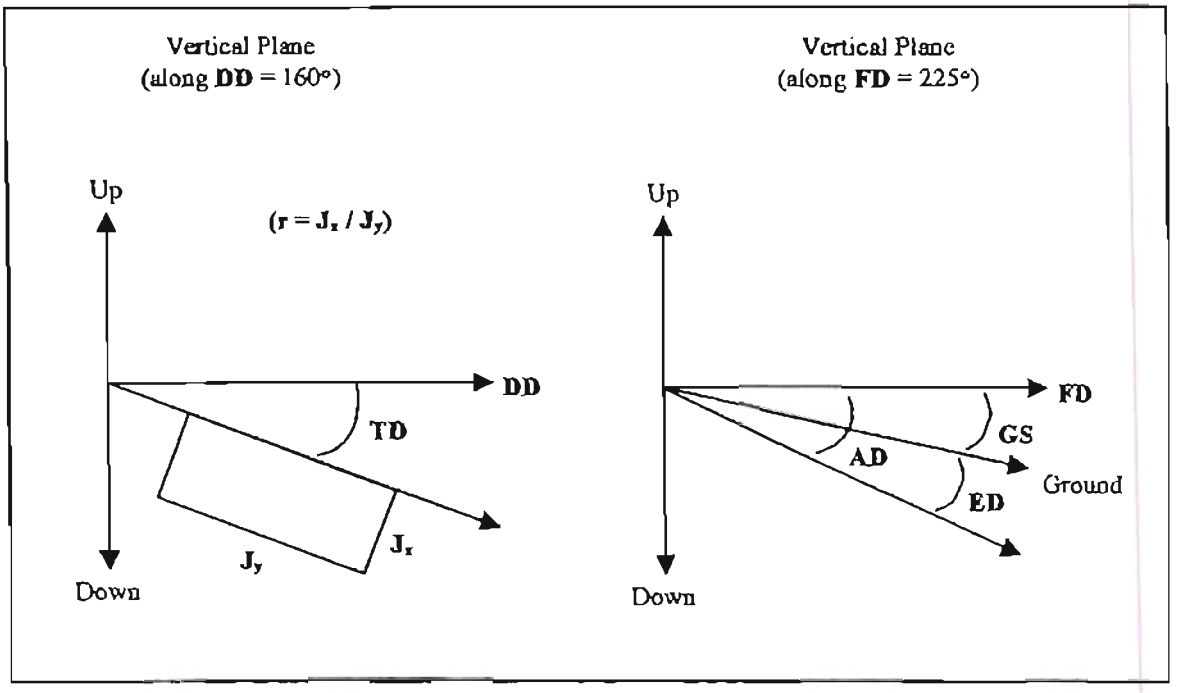

Figure 23. Vertical plane showing relationships between dip direction (*DD*), true dip (*TD*),

flow direction (*FD*), ground slope (*GS*), apparent dip (*AD*) and effective dip (*EF*).

Table 7. Relative ground structure number (J_s)

Dip Direction of Closer Spaced Joint Set (degrees)	Dip Angle of Closer Spaced Joint Set (degrees)	Ratio of Joint Spacing, r			
		1:1	1:2	1:4	1:8
180/0	90	1.14	1.20	1.24	1.26
In direction of stream flow	89	0.78	0.71	0.65	0.61
	85	0.73	0.66	0.61	0.57
	80	0.67	0.60	0.55	0.52
	70	0.56	0.50	0.46	0.43
	60	0.50	0.46	0.42	0.40
	50	0.49	0.46	0.43	0.41
	40	0.53	0.49	0.46	0.45
	30	0.63	0.59	0.55	0.53
	20	0.84	0.77	0.71	0.67
	10	1.25	1.10	0.98	0.90
	5	1.39	1.23	1.09	1.01
	1	1.50	1.33	1.19	1.10
0/180	0	1.14	1.09	1.05	1.02
Against direction of stream flow	-1	0.78	0.85	0.90	0.94
	-5	0.73	0.79	0.84	0.88
	-10	0.67	0.72	0.78	0.81
	-20	0.56	0.62	0.66	0.69
	-30	0.50	0.55	0.58	0.60
	-40	0.49	0.52	0.55	0.57
	-50	0.53	0.56	0.59	0.61
	-60	0.63	0.68	0.71	0.73
	-70	0.84	0.91	0.97	1.01
	-80	1.26	1.41	1.53	1.61
	-85	1.39	1.55	1.69	1.77
	-89	1.50	1.68	1.82	1.91
180/0	-90	1.14	1.20	1.24	1.26

Notes: 1. For intact material take $J_s = 1.0$
2. For values of r greater than 8 take J_s as for r = 8

If the flow direction is not in the direction of the true dip, $\left(90^\circ \le |DD\text{-}FD| \le 270^\circ\right)$, the effective dip is determined by adding the ground slope to the apparent dip:

$$ED = AD + GS \tag{20}$$

Once the effective dip, the direction of the effective dip relative to the flow direction (with or against), and the joint spacing ratio have been determined, use table 7 to determine J_s. When working with intact material, such as massive rock or fine-grained massive clay, the value of J_s is 1.0. In cases where the value of r is greater than 8, use the values of J_s for $r = 8$.

CASE STUDY: WOODROW WILSON BRIDGE

The Woodrow Wilson Bridge over the Potomac River is an essential part of local, regional and national transportation systems (figure 24). The bridge carries six lanes of Capital Beltway traffic between Alexandria, Virginia and Oxon Hill, Maryland and is the last river crossing for approximately 80.5 km down river. Congestion and the frequency of drawbridge openings for marine traffic cause traffic delay at the bridge. The Woodrow Wilson Bridge is one of a few on the Interstate highway system that contains a movable span. Under current Coast Guard regulations, the 15.2 m high drawbridge opens approximately 240 times per year to allow for the passage of marine traffic traveling the Potomac River.

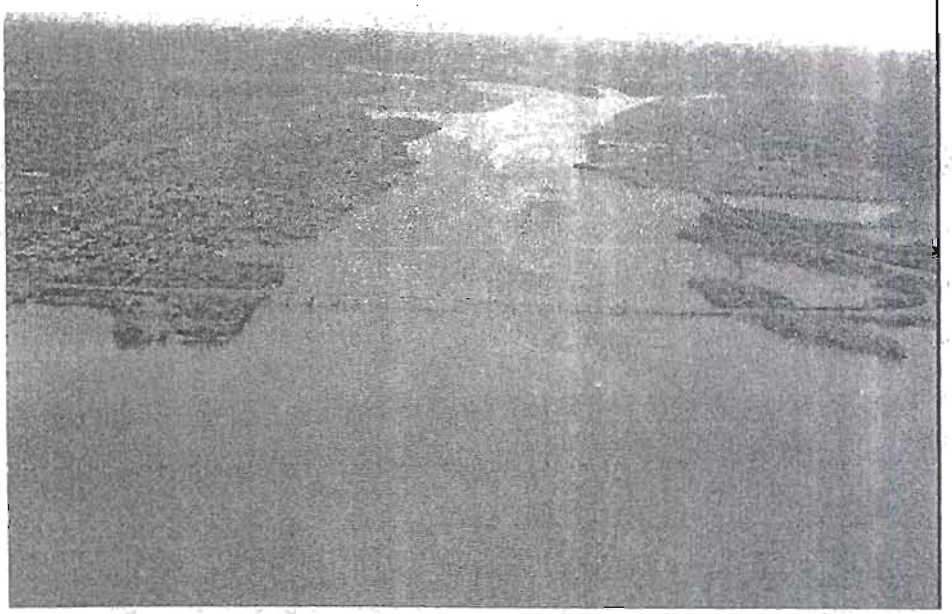

Figure 24. Potomac River and the existing Woodrow Wilson bridge. Virginia is on the left side of the bridge; Maryland is on the right side of the bridge.

The five-mile section of the Beltway within the project area serves as a systematic link for local traffic on major north-south roadways feeding into interchanges at Telegraph Road, US Route 1, I-295 and MD 210. Furthermore, the eastern half of the Beltway, including the Woodrow Wilson Bridge, is designated as I-95 and constitutes a critical link in the Maine to Florida Interstate route. Because the adjacent section of the hectic Beltway is eight lanes wide, the current six-lane Woodrow Wilson Bridge represents a severe bottleneck on the highway system.

Furthermore, the existing Woodrow Wilson Bridge cannot last much beyond 2004 without major structural rehabilitation. The inspections and repair activities at the Bridge would result in extended traffic delays and increased costs. Replacing the bridge before 2004 will greatly reduce traffic delays in the area.

In 1992, a Coordination Committee of affected jurisdictions from Maryland, Virginia, and the District of Columbia and local, regional, state and federal governments began investigating solutions to the traffic problems at Woodrow Wilson Bridge. The Committee approved a "Preferred Alternative" in 1996, which featured a facility with side-by-side, movable span, twin bridges with a 21.3 m navigational clearance. The new twin bridges will carry 10 lanes of traffic plus two future High Occupancy Vehicle (HOV) lanes. The new bridge design will clear the river by 21.3 m, which will reduce the number of openings by more than two-thirds, thus decreasing traffic delays.

This case study summarizes the procedure followed to estimate scour with the Erodibility Index Method at the proposed Woodrow Wilson Bridges. The analysis entailed assessment of riverbed material properties, hydraulic analysis and scour analysis as outlined in this paper. Potential scour depths for the 100-year and 500-year floods were calculated for each of the proposed bridge piers (see figure 25 for schematic of bridge pier layout). Factors of safety against scour were also calculated.

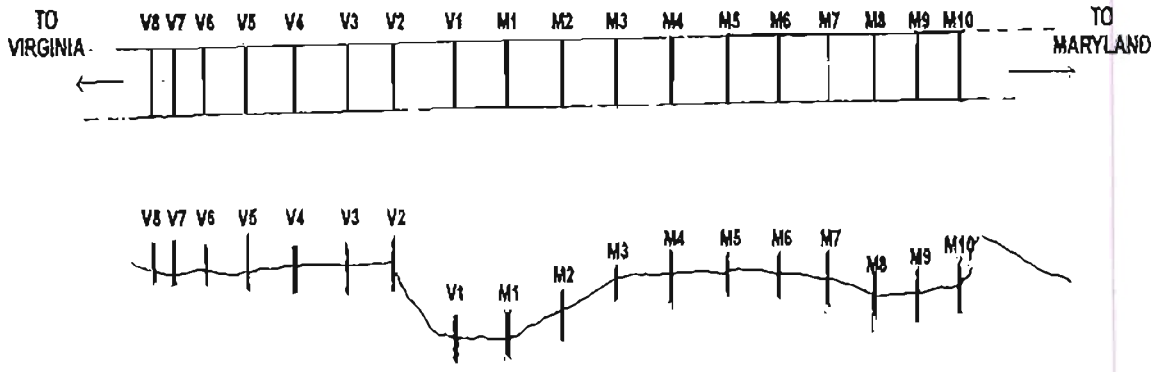

Figure 25. Schematic of bridge pier layout.

Riverbed Material Properties and Required Stream Power

Borehole logs, and shear strength and dilatometer test results were used to calculate the Erodibility Index of the riverbed. Boreholes, drilled near all of the proposed bridge piers, provided soil property information through descriptions and blow counts. Soil profiles near piers V1 and M1 through M5 have a thick layer of very soft to soft gray to brown silty clay, with some sand and gravel. Below is a layer of Pleistocene era terrace deposits, which are gray and brown, dense to very dense sand with silt, gravel and clay lenses. Finally, the Cretaceous period Potomac group consists of hard gray clay. Soil profiles near piers M6 through M10 and V2 have a thinner layer of soft to very soft alluvial clay, followed by a thin layer of alluvial deposits that consist of loose medium dense brown silty sand. The Pleistocene terrace deposits and Cretaceous Potomac group deposits follow. Dilatometer test results were used to estimate the undrained shear strength of the soil and the residual angle of friction. The shear strength test results were used to confirm the estimates made with the dilatometer test results.

Estimates of parameter values for the intact material strength number (M_s), the block or particle size number (K_b), the discontinuity or inter-particle bond shear strength number (K_d) and the relative shape and orientation number (J_s) were required to estimate the Erodibility Index. Estimation of each of these for the Woodrow Wilson Bridge are summarized in what follows.

Intact Material Strength Number (M_s)

In-situ dilatometer test (DMT) results were used to determine a relationship between depth and undrained shear strength of the very soft to soft clay material. A relationship was developed for the soft clay deposits, which begin at the riverbed surface and extend to various depths throughout the bridge cross-section of the riverbed. The soft and very soft alluvial deposits layer was estimated to have a cohesive intercept of 3.5 kPa and a residual angle of friction, ϕ, is 8.1°. The simplified relationship between undrained shear strength and depth below the original ground surface is:

$$Su = 3.5 + 1.42 \cdot H \tag{21}$$

where Su = undrained shear strength of soft and very soft alluvial deposits (kPa) and H = depth to the point in question from the original ground surface (m).

For borehole depths where the very soft to soft clay was found, equation (7) was used to calculate the undrained shear strength. The intact material strength number for cohesive soils can be calculated with the following equation (NRCS 1997),

$$M_s = 0.78 \cdot (UCS)^{1.09} = 0.78 \cdot (2 \cdot Su)^{1.09} \tag{22}$$

where UCS = unconfined compressive strength (MPa), which must be less than 10 MPa for this equation to be valid.

The intact material strength number for non-cohesive granular material was based on SPT blow counts and values from table A-1 in Annandale (1995).

For pier M10 column (3) of table 8 shows the value of Su (kPa) or the SPT blow count, whichever is applicable according to the log, at various depths below the riverbed surface. Note that Su values appear as decimal numbers; blow counts appear as whole numbers. Column (4) of table 8 shows the estimated values of M_s.

Block or Particle Size Number

The borehole log material descriptions were used to determine the particle/block size number, K_b. K_b was assigned a value of one for all materials except the hard clay. The hard clay of the cretaceous period Potomac group was assigned a value of 100. The reason for using $K_b = 100$ for the cretaceous period clay is that the clay is so hard that it can be viewed as soft intact rock according to tables in Annandale (1995). K_b determinations for pier M10 are shown in column (5) of table 8.

Discontinuity or Inter-particle Bond Shear Strength Number

The shear strength number, K_d, was calculated using the following equation (Annandale 1995):

$$K_d = \tan(\phi) \tag{23}$$

where $\phi = 8.1°$ for the very soft to soft clay material, but = 30° for all other materials. K_d values with depth for pier M10 are shown in table 8 column (6).

Relative Shape and Orientation Number

A value of one was assigned to the ground structure number, J_s, in all cases (Annandale 1995). J_s is shown in column (7) of table 8.

Table 8. Pier M10 calculations for available and required stream power for scour determination.

									100-Year Flood					500-Year Flood				
(1)	(2)	(3)	(4)	(5)	(6)	(7)	(8)	(9)	(10)	(11)	(12)	(13)	(14)	(15)	(16)	(17)	(18)	(19)
Depth, H (m)	Elevation (m)	Su (kPa) OR SPT	Ms	Kb	Kd	Js	EI	Required Stream Power (KW/m^2)	Dimension-less scour depth	Relative Stream Power	Available Stream Power (KW/m^2)	P_R/P_A	Scour (Y/N) ?	Dimension-less scour depth	Relative Stream Power	Available Stream Power (KW/m^2)	Scour (Y/N) ?	P_R/P_A
0	-0.728	3.5	0.003	1	0.142	1	0.000	0.017	0					0				
0.305	-1.033	3.933	0.004	1	0.142	1	0.001	0.018	0.018	8.15	0.0784	0.23	yes	0.016	14.12	0.3381	yes	0.05
0.610	-1.338	4.366	0.004	1	0.142	1	0.001	0.019	0.036	7.88	0.0758	0.25	yes	0.032	13.55	0.3247	yes	0.06
0.914	-1.643	4.798	0.005	1	0.142	1	0.001	0.020	0.054	7.62	0.0733	0.27	yes	0.047	13.02	0.3118	yes	0.06
1.219	-1.948	5.231	0.005	1	0.142	1	0.001	0.020	0.071	7.36	0.0709	0.29	yes	0.063	12.50	0.2994	yes	0.07
1.524	-2.252	5.664	0.006	1	0.142	1	0.001	0.021	0.089	7.12	0.0685	0.31	yes	0.079	12.00	0.2875	yes	0.07
1.829	-2.557	6.097	0.006	1	0.142	1	0.001	0.022	0.107	6.88	0.0662	0.33	yes	0.095	11.52	0.2760	yes	0.08
2.134	-2.862	6.530	0.007	1	0.142	1	0.001	0.023	0.125	6.66	0.0641	0.36	yes	0.111	11.06	0.2650	yes	0.09
2.438	-3.167	6.963	0.007	1	0.142	1	0.001	0.023	0.143	6.44	0.0619	0.38	yes	0.126	10.62	0.2545	yes	0.09
2.743	-3.472	7.395	0.008	1	0.142	1	0.001	0.024	0.161	6.22	0.0599	0.40	yes	0.142	10.20	0.2444	yes	0.10
3.048	-3.777	7.828	0.008	1	0.142	1	0.001	0.025	0.179	6.02	0.0579	0.43	yes	0.158	9.80	0.2347	yes	0.11
3.353	-4.081	8.261	0.009	1	0.142	1	0.001	0.026	0.196	5.82	0.0560	0.46	yes	0.174	9.41	0.2253	yes	0.11
3.658	-4.386	8.694	0.009	1	0.142	1	0.001	0.026	0.214	5.62	0.0541	0.48	yes	0.190	9.03	0.2164	yes	0.12
3.962	-4.691	9.127	0.010	1	0.142	1	0.001	0.027	0.232	5.44	0.0523	0.51	yes	0.205	8.67	0.2077	yes	0.13
4.267	-4.996	9.559	0.010	1	0.142	1	0.001	0.027	0.250	5.26	0.0506	0.54	yes	0.221	8.33	0.1995	yes	0.14
4.572	-5.301	2	0.01	1	0.577	1	0.007	0.053	0.268	5.08	0.0489	1.08	no	0.237	8.00	0.1915	yes	0.28
4.877	-5.605	2	0.01	1	0.577	1	0.007	0.053	0.286	4.92	0.0473	1.12	no	0.253	7.68	0.1839	yes	0.29
5.182	-5.910	2	0.01	1	0.577	1	0.007	0.053	0.304	4.75	0.0457	1.16	no	0.269	7.37	0.1766	yes	0.30
5.486	-6.215	2	0.01	1	0.577	1	0.007	0.053	0.321	4.60	0.0442	1.20	no	0.284	7.08	0.1696	yes	0.31
5.791	-6.520	2	0.01	1	0.577	1	0.007	0.053	0.339	4.44	0.0428	1.24	no	0.300	6.80	0.1628	yes	0.33
6.096	-6.825	1	0.01	1	0.577	1	0.003	0.040	0.357	4.30	0.0414	0.96	yes	0.316	6.53	0.1564	yes	0.25
6.401	-7.129	1	0.01	1	0.577	1	0.003	0.040	0.375	4.15	0.0400	0.99	yes	0.332	6.27	0.1501	yes	0.26
6.706	-7.434	1	0.01	1	0.577	1	0.003	0.040	0.393	4.02	0.0387	1.03	no	0.348	6.02	0.1442	yes	0.28
7.010	-7.739	1	0.01	1	0.577	1	0.003	0.040	0.411	3.88	0.0374	1.06	no	0.363	5.78	0.1384	yes	0.29
7.315	-8.044	1	0.01	1	0.577	1	0.003	0.040	0.429	3.76	0.0361	1.10	no	0.379	5.55	0.1329	yes	0.30
7.620	-8.349	20	0.07	1	0.577	1	0.042	0.119	0.446	3.63	0.0349	3.40	no	0.395	5.33	0.1276	yes	0.93
7.925	-8.653	20	0.07	1	0.577	1	0.042	0.119	0.464	3.51	0.0338	3.52	no	0.411	5.12	0.1226	yes	0.97
8.230	-8.958	20	0.07	1	0.577	1	0.042	0.119	0.482	3.40	0.0327	3.64	no	0.427	4.91	0.1177	no	1.01
8.534	-9.263	20	0.07	1	0.577	1	0.042	0.119	0.500	3.28	0.0316	3.76	no	0.442	4.72	0.1130	no	1.05
8.839	-9.568	20	0.07	1	0.577	1	0.042	0.119	0.518	3.17	0.0305	3.89	no	0.458	4.53	0.1085	no	1.10
9.144	-9.873	14	0.06	1	0.577	1	0.033	0.107	0.536	3.07	0.0295	3.62	no	0.474	4.35	0.1042	no	1.03
9.449	-10.177	14	0.06	1	0.577	1	0.033	0.107	0.554	2.97	0.0286	3.75	no	0.490	4.18	0.1000	no	1.07

Erodibility Index and Required Power

Erodibility Index (EI), the product of Ms, Kb, Kd, and Ks, is shown in table 8 column (8). The power required to scour the Potomac River's bed material was determined using Annandale's (1995) erosion threshold (Wittler, et al. 1998) for low strength materials (as a conservative approach):

$$pR = 0.48 \cdot EI^{0.44} \tag{24}$$

where pR = power required to scour granular material (kW/m2). Required stream power is calculated in table 8 column (9) for pier M10.Available Stream Power

The available stream power at each proposed bridge pier was determined with HEC-RAS model results. The available power around the bridge piers was expressed as a function of scour hole depth and quantified through a three-step process using the available data.

First, the available stream power of the Potomac River at a point upstream of the proposed bridge was calculated for each proposed pier using:

$$P_a = \gamma \cdot v \cdot d \cdot s \tag{25}$$

where P_a = available stream power in the river upstream of a bridge pier (kW/m^2); γ = unit weight of water (kN/m^3); v = velocity of water (m/s); d = flow depth (m); and s = energy slope of flow in the river. Data for approach velocity, depth of flow, and energy slope in the Potomac River were obtained from the HEC-RAS model for a river section approximately 1.5 m upstream of the proposed Woodrow Wilson Bridge. The HEC-RAS model was designed to calculate a velocity distribution across the river cross-section, thus allowing velocity upstream of each proposed pier to be approximated. The number of HEC-RAS model flow tubes affected the velocity calculated at the piers; thus the number of tubes was varied to achieve maximum velocities at the bridge piers. A schematic of velocity across the upstream section is shown in figure 26. Available stream power upstream of the bridge was calculated for the HEC-RAS data for the 100-year

and 500-year floods. Hydraulic data and resulting available stream power are presented in table 9 for pier M10.

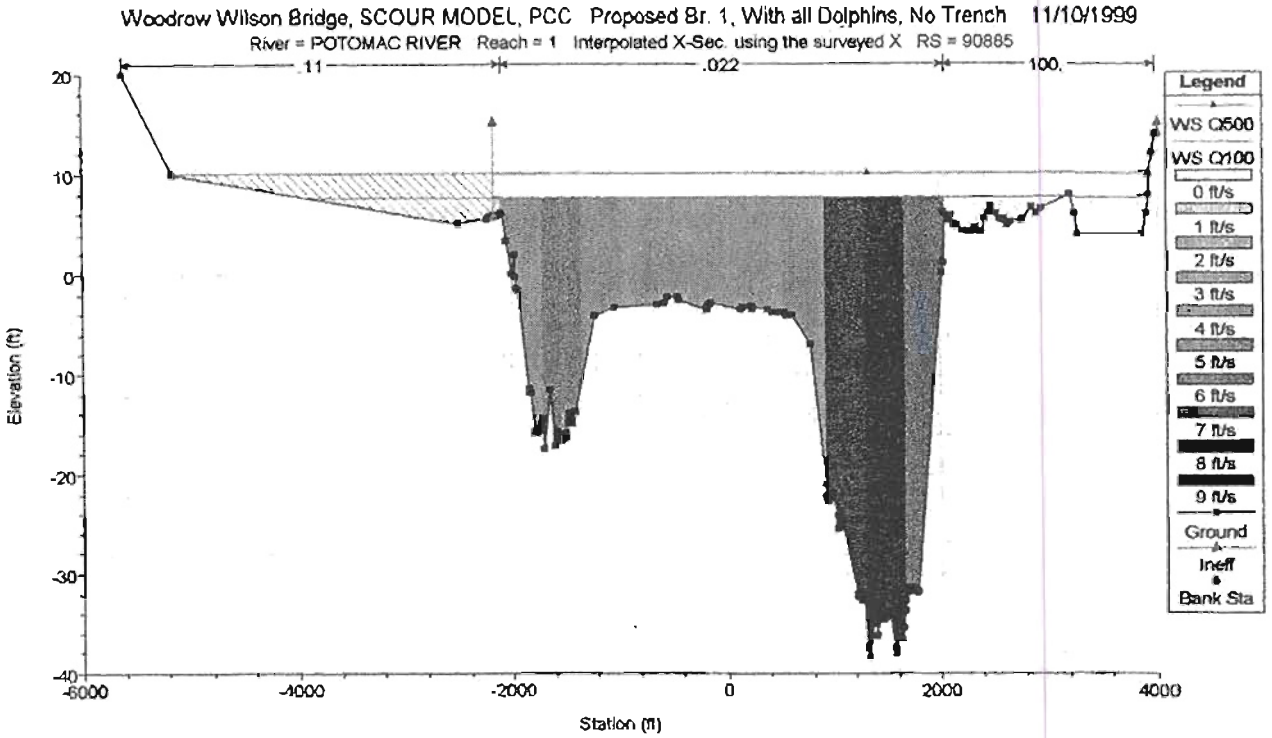

Figure 26. Velocity distribution from HEC-RAS model of Potomac River at cross-section approximately 5 mi upstream of the proposed bridges.

Table 9. Pier M10 Hydraulic Data.

Hydraulic Variable	100-Year Flood	500-Year Flood
Upstream Velocity	3.98 fps =1.21 m/s	5.49 fps = 1.67 m/s
Water Surface Elev.	10.86 ft = 3.31 m	14.69 ft = 4.48 m
Ground Surface Elev.	-2.39 ft = -0.73 m	-2.39 ft = -0.73 m
Flow Depth	13.25 ft = 4.04 m	17.08 ft = 5.21 m
Gamma	9.82 kN/m^3	9.82 kN/m^3
Energy Slope	0.0002	0.00028
Upstream Stream Power	0.010 kW/m^2	0.024 kW/m^2
HEC-18 Scour Depth	56.0 ft = 17.1 m	63.3 ft = 19.3 m

In the second step, a relationship between dimensionless stream power at the base of a scour hole and dimensionless scour hole depth was determined using figure 11. The stream power is expressed in dimensionless form on the ordinate of the graph as the ratio P/Pa and scour depth as

the ratio ys/ymax. Pa is the magnitude of the stream power in the river upstream of the pier as determined by equation (4), and P is the magnitude of the stream power at the base of the scour hole as it increases in depth. The variable ymax represents the maximum scour depth that can develop around a bridge pier under given flow conditions, whereas ys represents variable scour depth (ys < ymax). The maximum depth was assumed to be that calculated by HEC-18.

The equations used to make figure 11 dimensional are:

$$\text{Rectangular Piers:} \quad P / P_a = 8.42 \cdot e^{-1.88 \cdot (y_s / y_{max})}, \tag{26a}$$

$$\text{Circular Dolphins:} \quad P / P_a = 8.95 \cdot e^{-1.92 \cdot (y_s / y_{max})}, \tag{26b}$$

The dimensionless scour depths for pier M10 are shown in table 8 columns (10) and (15) for the 100- and 500-year floods, respectively. Columns (11) and (16) of table 8 show 100- and 500-year flood relative stream power calculations using equation (26a) for pier M10.

In step three, the available stream power at a given scour depth, P (subsequently referred to as pA), is the product of P_a from step one and P/P_a from step two. The pA calculations for pier M10 are shown in table 8 columns (12) and (17) for the 100- and 500-year floods, respectively.

Results and Discussion for Example Pier M10

The scour elevation at pier M10 was determined by comparing the stream power that is available to cause scour, pA, and the stream power that is required to scour the riverbed material, pR. Scour is expected to occur until pA is less than pR. Available power and required power are shown versus elevation in figure 27. Table 8 columns (14) and (18) for the 100- and 500-year floods, respectively, show whether scour is expected to occur at a given elevation. For the 100-year flood, scour is expected to occur to a depth of 4.6 m, which is an elevation of –5.3 m. The calculated scour depth for the 500-year flood is 8.2 m (elevation of –8.96 m). The Erodibility Index Method predicted scour elevations at pier M10 are 12.5 m and 11 m shallower than the HEC 18 predictions for the 100- and 500-year floods, respectively.

The factor of safety quantifies the ability of the earth material to withstand the erosive power of the river at potential scour depths. The factor of safety was calculated as the required stream power divided by the available stream power in columns (13) and (19) of table 8 for pier M10. The factor of safety at the base of the expected 100-year flood scour hole is approximately 1.

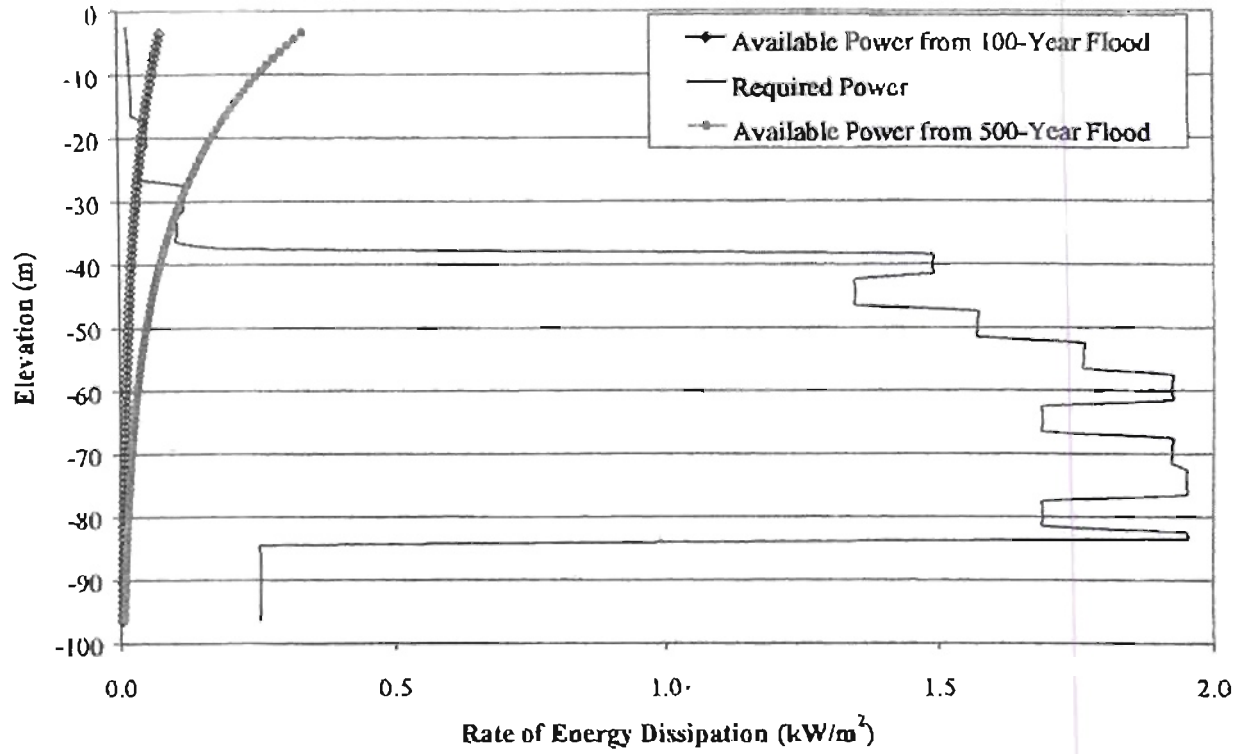

Figure 27. Available stream power and power required at pier M10.

The variation in the factors of safety with depth, as seen in table 8, is dictated by the relationship between the variation in material properties as a function of elevation below the riverbed and changes in the available stream power. To be conservative in the bridge pier design, Maryland State Highway Department is designing pier M10's foundation at the elevation where the 500-year flood factor of safety is greater than 5.0; this elevation is 11.7 m with a factor of safety of 18.3.

REFERENCES

1. Anglio, C.D., Nairn, R.B., Cornett, A.M., Dunaszegi, L., Turnham, J. and Annandale, G.W., 1996, Bridge Pier Scour Assessment for the Northumberland Strait Crossing, Coastal Engineering 1996, *Proceedings of the Twenty-fifth International Conference held in Orlando*, Florida, September 2-6, 1996, Billy L. Edge, Editor.

2. Annandale, G. W., Wittler, R. J., Ruff, J. F. and Lewis, T. M., 1998, Prototype Validation of Erodibility Index for Scour in Fractured Rock Media, Proceedings of the Water Resources Conference, American Society of Civil Engineers, Memphis, Tennessee, August.

3. Annandale, G.W., 1995, "*Erodibility.*" Journal of Hydraulic Research, Vol. 33, No. 4, pp. 471-494.

4. Briaud, J-L, Ting, F.C.K., Chen, H.C., Gudavalli, R. Perugu, S. and Wei, G., 1999, SRICOS: Prediction of Scour Rate in Cohesive Soils at Bridge Piers, Journal of Geotechnical and Geoenvironmental Engineering, American Society of Civil Engineers, Vol. 125, No. 4.

5. Cohen, E. and Von Thun, J. L., 1994, Dam Safety Assessment of the Erosion Potential of the Service Spillway at Bartlett Dam, *Proc. International Commission on Large Dams*, Durban, South Africa, pp. 1365-1378.

6. Federal Highway Administration, 1995, Evaluating Scour at Bridges, Third Edition, Hydraulic Engineering Circular 18 (HEC-18), Publication No. FHWA-IP-90-017, US Department of Transportation, 400 Seventh Street, Washington D.C. 20590.

7. Hjulstrom, F., 1935, The Morphological Activity of Rivers, Bulletin of the Geological Institute, Uppsala, Vol. 25, chapter 3.

8. Kirsten, H.A.D., 1982, A classification system for excavation in natural materials, *The Civil Engineer in South Africa*, July, pp. 292-308.

9. Shields, A., 1936, Application of Similarity Principles and Turbulence Research to Bed-Load Movement (in German), Mitteilungen der Preuss. Versuchsanstalt fur Wasserbau und Schiffbau, Berlin, No. 26.

10. Smith, S. P., Annandale, G. W., Johnson, P. A., Jones, J. S. and Umbrell, E. R., 1997, "Pier Scour in Resistant Material: Current Research on Erosive Power", Proceedings of Managing Water: Coping with Scarcity and Abundance, 27th Congress of the International Association of Hydraulic Research, San Francisco, California, pp. 160-165.

11. U.S. Natural Resources Conservation Service (NRCS), 1997, *Field procedures guide for the headcut erodibility index*, Chapter 52, in "Part 628 : Dams" of the National Engineering Handbook. Washington D.C. : U.S. Department of Agriculture.

12. Wittler, R.J., Annandale, G.W., Abt, S.R., Ruff, J.F., 1998, "New Technology for Estimating Plunge Pool or Spillway Scour." *Proceedings of the 1998 Annual Conference of the Association of State Dam Safety Officials*. October 11-14, Las Vegas, NV.

13. Yang, C. T., 1973, Incipient Motion and Sediment Transport, Journal of the Hydraulics Division, ASCE, Vol. 99, No. HY10, Proceedings Paper 10067, pp. 1679-1704.